Gordan Sipka, BSc

Calibration and Verification Methodology in Production Environment for 13.56 MHz RFID Applications

Master's Thesis

to achieve the university degree of

Diplom-Ingenieur

Master's degree programme: Electrical Engineering

submitted to

Graz University of Technology

Ass. Prof. Dipl.-Ing. Dr.techn. Peter Söser

Institute of Electronics
Inffeldgasse 12/I
A - 8010 Graz, Austria

in Cooperation with

Infineon Technologies Austria AG

Advisor: Dipl.-Ing.Ing. Georg Skacel, BSc

Affidavit

I declare that I have authored this thesis independently, that I have not used other than the declared sources/resources, and that I have explicitly indicated all material which has been quoted either literally or by content from the sources used. The text document uploaded to TUGRAZonline is identical to the present master's thesis.

Date

Signature

Danksagung

Mein besonderer Dank gilt der Infineon Technologies Austria AG für das Ermöglichen dieser Arbeit. Vor allem meiner Abteilung STM unter der Leitung von Roman Kurzman, die mich herzlich aufgenommen hat und mir die Gelegenheit gab, mich weiterzubilden und an interessanten Themengebieten mitzuwirken.

Ein herzlicher Dank gilt meinem Kollegen und Mentor, Georg Skacel, der mich mit all seinen Mitteln unterstützte und ohne dessen Hilfe und Bemühungen diese Arbeit nicht zustande gekommen wäre. Seine Unterstützung und seine Geduld ermöglichten es, diese Arbeit zu vollenden.

Weiters möchte ich mich bei meinem Betreuer Ass. Prof. Peter Söser vom Institut für Elektronik der Technischen Universität Graz für die intensive und sehr herzliche Betreuung bedanken.

An dieser Stelle möchte ich mich auch bei all meinen Freunden bedanken, die mich während meiner Studienzeit begleitet und bei der Erstellung dieser Arbeit unterstützt haben.

Vielen Dank an meine Familie für ihre großartige und wertvolle Unterstützung in der Studienzeit und dafür, dass sie mir auch in schwierigen Zeiten immer zur Seite standen und mich zu dem Menschen geprägt haben, der ich heute bin. Ein besonderer Dank geht an meine Gattin, Maida und unsere Töchter, Sara und Maja. Ihr habt einen wichtigen Beitrag geleistet und mir so viel Kraft während meiner Studienzeit geschenkt. Ich danke euch von ganzem Herzen.

Abstract

This master thesis developed the design and implementation of the Automated Diagnostic Tool (ADT). The general purpose of ADT is to check verification and calibration of the Test System (TS). In the semiconductor industry quality assurance needs to be established during the production process. The ADT offers the possibility in the production process to face discrepancies or problems quickly and suggest solutions or improvements in time. In this study I proposed a deeper TS analysis which consists of important hardware parameters that will determine the requirements for ADT as well as the measuring instruments that are necessary for the calibration of the TS.

The most important contribution is that I conducted in-depth case studies of the ADT to prove its functionality and relevance. I tested this prototype by using established methods of testing and measuring.

The major findings from the research illustrate how the ADT will allow to effectively reduce failure searching times, as failures can be found and diagnosed very easily in this process. The findings provide support for the key arguments that this prototype is essential to the expert support and cuts the cost of high maintenance.

Kurzfassung

Das Ziel dieser Masterarbeit ist die Entwicklung und die Implementierung des Automated Diagnostic Tools (ADT). Die allgemeine Aufgabe des ADTs ist die Überprüfung der Verifizierung und Kalibrierung des Test System (TS)s. In der Halbleiterindustrie ist es notwendig während des Produktionsprozesses die Qualitätssicherungssmaßnahmen einzuhalten und zu dokumentieren. Das ADT bietet die Möglichkeit im Produktionsprozess schnell Fehlfunktionen des TS zu erkennen und eine entsprechende Lösung oder Fehlerbehebung vorzuschlagen. In dieser Studie wurde eine detaillierte Analyse des TSs durchgeführt, durch dessen Resultat sich die Anforderungen an das ADT definiert haben. Ein weiteres Resultat war die Bestimmung der Messinstrumente, die für die Kalibrierung des TSs erforderlich sind.

Der wichtigste Beitrag ist, dass eingehende Fallstudien zum ADT durchgeführt wurden, um die Funktionalität und Relevanz zu beweisen. Der Prototyp wurde mit etablierten Test- und Messmethoden erprobt und verifiziert. Weitere Tests mit Hilfe des realen TSs haben die Fähigkeiten und die Zuverlässigkeit des ADTs demonstriert und bewiesen.

Die Ergebnisse der Untersuchungen zeigen, wie das ADT die Fehlersuchzeiten effektiv reduzieren kann, da Fehler sehr leicht gefunden und diagnostiziert werden können. Die Ergebnisse unterstützen das Hauptargument, dass dieser Prototyp für die fachliche Unterstützung und kompetente Betreuung unerlässlich ist und gleichzeitig einen Beitrag zur Kostenoptimierung im laufenden Betrieb leisten kann.

Glossary

GPIO General Purpose Input Output
GUI Graphical User Interface
IC Integrated Circuit
I²C Inter-Integrated Circuit
IO Input Output
PCB Printed Circuit Board
PCD Proximity Coupling Device
PICC Proximity Integrated Chip Card
RFID Radio-Frequency Identification
VNA Vector Network Analyzer
TS Test System
ADT Automated Diagnostic Tool
DMM Digital Multi Meter
SMU Source Measure Unit
PTC Positive Temperature Coefficient
SPST Single Pole Single Throw
FG Function Generator
SDA Serial Data Line
SCL Serial Clock Line
ACK Acknowledge
DUT Device Under Test

Contents

List of Figures

List of Tables

1 Introduction

1.1 Motivation

Quality affects the continuity and the rhythm of production in many ways, together with production costs, production volume and workforce productivity. In the semiconductor industry, quality assurance is a very important topic. Quality assurance works hand in hand with production in order to tackle discrepancies or problems quickly and offer solution approaches or improvement suggestions at any time. Companies invest a lot of effort to provide their customers with the best possible quality. In order to ensure such quality, it is necessary for the products to be subjected to a final contactless test once more before their delivery. Contactless testing is required to make sure that the components are compliant with their specifications, and the whole contactless system works as expected.

Since there are no manufactured testing instruments for such output tests in the field of 13.56 MHz RFID systems, the companies must rely on themselves to find the solutions. For this reason, Infineon Technologies AG has developed a Test System (TS) in accordance with ISO/IEC 10373-6 standards that is completely controlled by industrial RFID readers. This TS is a measuring device specifically designed for the RFID technology. Together with the reel to reel handler, the TS forms a setup test for contactless RFID modules tests. The TS device has to be in contact with the RFID chip module via Pogo pins to perform testing, initialization and personalization of the RFID chip module. Like with every measuring device, a continuous verification and calibration of the TS is required.

1.2 Goals of the Thesis

In this regard, this thesis describes the design and implementation of the ADT. The general purpose of ADT is to check verification and calibration of the TS, particularly its hardware and root cause failure analysis, as well as to provide a solution for the identified errors.

A deeper TS analysis which consists of important hardware parameters will determine the requirements for ADT as well as the measuring instruments that are necessary for the calibration of the TS. Knowledge acquired from the evaluated parameters is to be subsequently confirmed through practical application of the Automated Diagnostic Tool and its relevance is to be assessed.

The ADT system developed for this thesis can be separated into three important segments:

1. **Hardware design**
2. **Enclosure design**
3. **Software design**

1.3 Structure of the Thesis

This thesis is organized in five chapters. Chapter 1 describes the motivation and objective of the master's thesis. Chapter 2 gives a basic overview of RFID technology and description of the hardware components as Raspberry Pi, Red Pitaya and miniVNA. Chapter 3 focuses on the System design, beginning with the requirements and system concept including the description of the single hardware components, enclosure design and software design. After its description, the system must be evaluated through testing and measurements. All of this is contained in chapter 4. The last chapter, chapter 5 offers a conclusion of the entire thesis and gives an outlook for the future.

2 Basics

2.1 RFID Basics

Radio Frequency Identification (RFID) uses electric and magnetic fields to achieve contactless identification procedures. RFID is a communication technology that allows stationary or moving objects to be identified wirelessly by means of magnetic or electromagnetic fields. The areas of application extend from article surveillance and detection systems, over to contactless chip cards, and up to person and animal identification. Typical RFID systems consist of the following elements (see Figure 2.1):

- a transponder (Proximity Integrated Chip Card (PICC), also referred to as tag = label) that stores data.
- a reader Proximity Coupling Device (PCD), which is able to read the data stored in the transponder.
- a computer system that collects the data coming from the reader, decrypts and evaluates it.

Data exchange can be performed in both directions. There are read and write accesses possible, which allow addition of new data or modification of existing data. In the data transfer between transponder and reader two different methods of energy supply are used: the duplex method and the sequential method. In the duplex method, the energy transfer during communication in both directions is continuous and independent of data transmission. In sequential systems, the energy flow to the transponder pauses when there is a data flow towards the reader. [10]

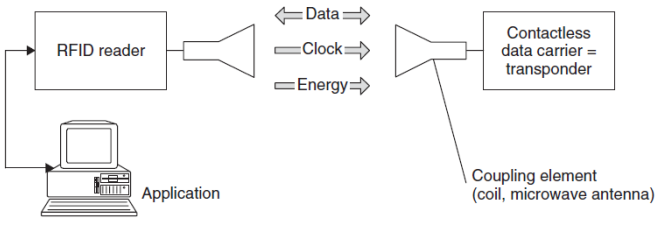

Figure 2.1: Main components of a RFID system

2.1.0.1 Transponder

Depending on the application, transponders can be designed differently. They usually contain an antenna and a microchip (see Figure 2.2). Transponders can be either passive,

active or battery-assisted passive. An active transponder has an on-board battery. A battery-assisted passive transponder (BAP) has a small battery on board and is activated in the presence of an RFID reader. A passive transponder has no battery and uses the radio energy transmitted by the reader. Meanwhile, many RFID tags have electronic microchips embedded on them. This allows information to be processed on the transponder itself. Many passive RFID systems are in use, because they are activated only by getting in contact with the reader. This renders the energy issue obsolete and the lack of any active power supply makes these systems cheaper. [10]

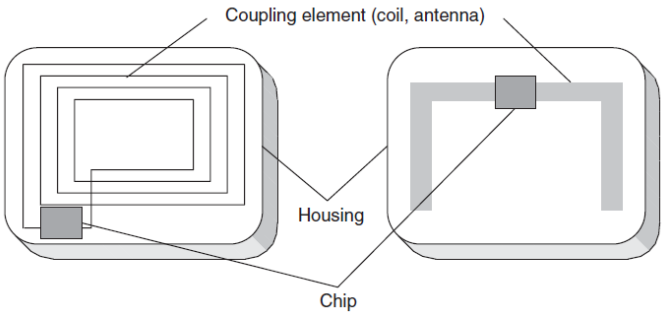

Figure 2.2: Main components of a Transponder

2.1.0.2 Reader

The reader is the base station of an RFID system and its design depends on the manufacturer and application (see Figure 2.3). Readers consist of a radio frequency unit (transmitter and receiver), a coupling element (antenna) to the transponder, and an interface to the evaluation system. In order to control the reader and send commands to the transponder, they are mostly equipped with various interfaces such as USB, Ethernet or RS-232. The size of the housing often depends on the installed coupling device. [16]

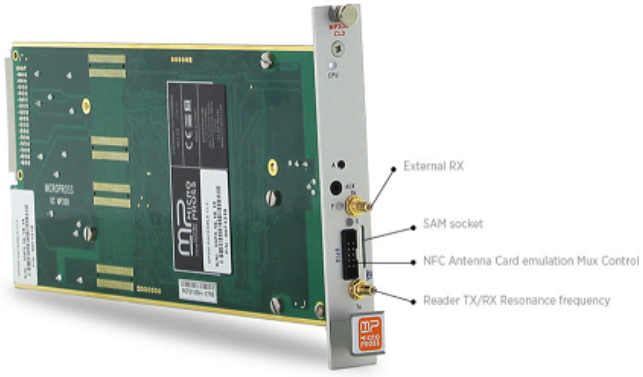

Figure 2.3: Contactless reader MP300 CL3 [19]

2.1.0.3 Classification of RFID Systems

Depending on the application a large number of different RFID systems are available on the market. The most important distinguishing attributes are: the operating frequency, the type of coupling between transponder and reader, and the resulting range.

- *Low-Frequency (LF) between 30 kHz and 300 kHz,*
- *High-Frequency (HF) systems are defined for frequencies between 3 MHz and 30 MHz and*
- *Ultra high Frequency (UHF) with frequencies between 300 MHz and 3 GHz.*

Range of RFID systems is divided into the following three categories:

- *close coupling systems:* In close coupling systems a range of approx. 1 cm is usually achieved, and they are used for high security applications. The operating frequency can be chosen from DC up to 30 MHz.
- *remote coupling systems:* Remote coupling systems operate at distances of up to 1 m and are most commonly based on inductive coupling. There are two sub-categories of remote coupling systems: proximity coupling and vicinity coupling systems. Typical transmission frequency values are 135 kHz or 13.56 MHz, with 27.125 MHz also being used in some special cases.
- *long range systems:* With long range systems, ranges higher than 1 m can be achieved. Frequencies are usually in the UHF (868 MHz and 915 MHz) or microwave (2.5 GHz and 5.8 GHz) range.

2.2 Description of the Hardware Components

2.2.1 Raspberry Pi

Raspberry Pi is a credit card sized single board computer that can be utilized for many purposes such as Desktop PC, for playing Audio and Video files as well as running commercial or industrial applications. The Raspberry Pi concept was invented in 2006 by Dr. Eben Upton and his colleagues at The Cambridge University Computer Laboratory, England. As a commercial product Raspberry Pi was launched by the nonprofit organization the Raspberry Pi Foundation. The Raspberry Pi 3 Modell B (see Figure 2.4) is the third generation Raspberry Pi. This powerful single board computer can be applicable to many usages and replaces the original Raspberry Pi Model B+ and Raspberry Pi 2 Model B.

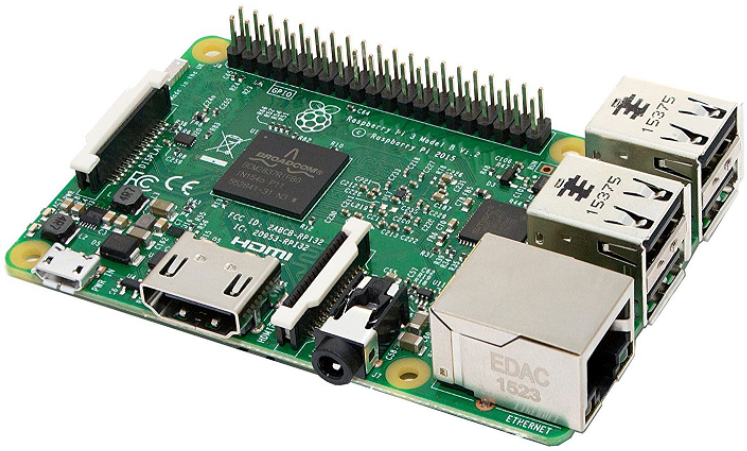

Figure 2.4: Raspberry Pi 3 Model B [11]

In order to preserve the beloved form of the board, the Raspberry Pi 3 Model B has a Quad-Core-Processor with 1.2 GHz of Broadcom and 1 GB SDRAM memory which is 10 times faster than the first generation Raspberry Pi. The Raspberry Pi 3 features a built-in WLAN compliant to IEEE 802.11 b/g/n combined with an on board Bluetooth Low Energy that do not require additional set up through external USB Adapter. This version has four USB ports, a 100 Mbit network jack, a HDMI port, an analog Audio output and Camera Serial Interface (CSI), specifically Display Serial Interface (DSI). Altogether, 40 General Purpose Input Output (GPIO) Pins that can be used beside generic Inputs and Outputs as well as special interfaces such as UART, I^2C and SPI are provided.

The Raspberry Pi is not like an ordinary computer with hard disk or SSD. Instead, the SD Card serves as a memory space for the operating system and the usersdata. The operating system is supported primarily with Raspbian, ARMv6 optimized version of

Debian. Furthermore, the downloadable versions of Arch Linux (Arch), Fedora (Pidora), XBMC (XBian, OpenElec, Raspbmc), RiscOS, Android and many other operating systems are available.

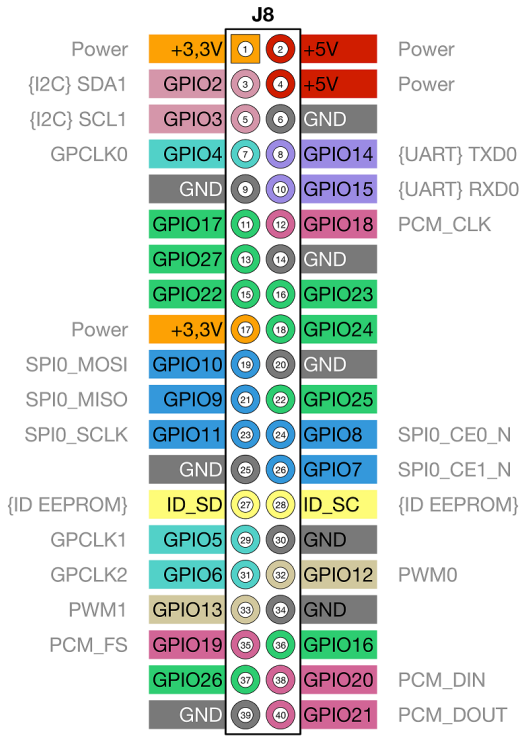

Figure 2.5: Raspberry Pi 3 Model B GPIO 40 Pin Block Pinout [11]

Due to the many connection options (see Figure 2.5), the large selection of communication interfaces, its processing power for real-time analyses and especially its good deal price, the Raspberry Pi is ideal for automation and control technology.

2.2.1.1 I²C Protocol Description

The I²C is a serial interface designed and developed by Philips Semiconductor. I²C is also called two wire interface protocol because it uses only two lines for the data transfer between devices, Serial Data Line (SDA) and Serial Clock Line (SCL). The I²C is a master/slave interface. That means there is at least one master-slave setup as shown in Figure 2.6. The master device controls the SCL line and initializes data transmissions from and to the slave device through the SDA line. It is possible to have multiple master devices connected to the bus. This multi master architecture will not be taken into consideration. [14]

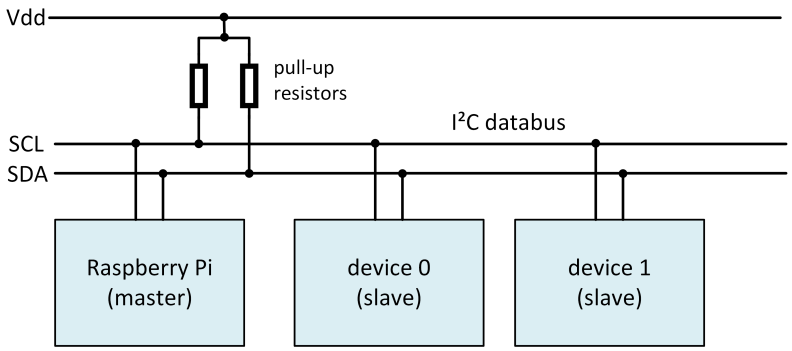

Figure 2.6: The Structure of I²C bus

All devices connected via a bus must have a unique address. Usually the I²C bus has a 7-bit or a 10-bit address. This addressing scheme allows the master device to connect a specific slave device. Both, start and stop conditions are generated by the master device. In the start condition, the master is informing all the slaves that something is going to be transmitted on the I²C lines, SDA line is pulled down while the SCL remains high (see Figure 2.7). [14]

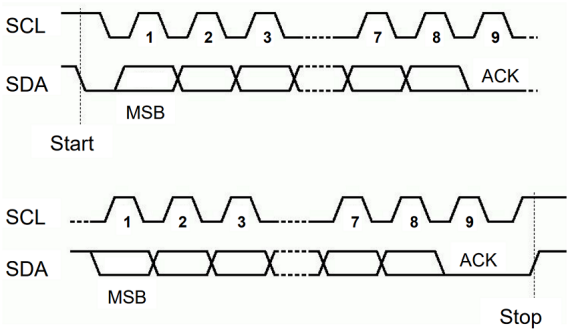

Figure 2.7: Start condition and stop condition

After sending the start bit the master sends the 7-bit address of the slave device. When the master sends a bit with a logical value 0, it represents a write operation. Write operation means that the master device writes data on the bus and a slave device reads data from the bus. If the master sends a bit with a logical value 1, it represents a read operation. Read operation means that the master device reads data from the bus and a slave device writes data on the bus. After each data byte the slave responds with the conformation Acknowledge (ACK).

When the transmission of the data between master and slave is completed, the master issues a stop condition and the bus becomes idle. This is done by releasing the SCL line followed by SDA line. Both lines must be connected via a Pull-up resistor to Vcc. Theses Pull-up resistors are needed because the I²C bus is an open drain technology. This means, when in idle state the Pull-up resistors that are connected with the lines increase the voltage. [14]

The data transfer from master to slave is shown in Figure 2.8. Furthermore, it can be seen how the SDA bus line is used for the data transfer. The value of the R/W bit is 0 and this value representing a write operation.

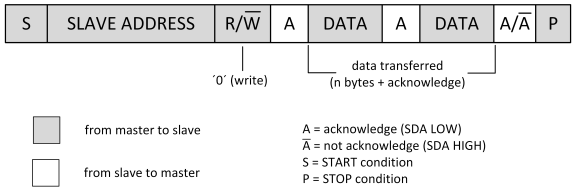

Figure 2.8: Data transfer from master to slave

The data transfer from slave to master is shown in Figure 2.9. In addition, it can be seen how the SDA bus line is used for the data transfer. The value of the R/W bit is 1 and this value representing a read operation.

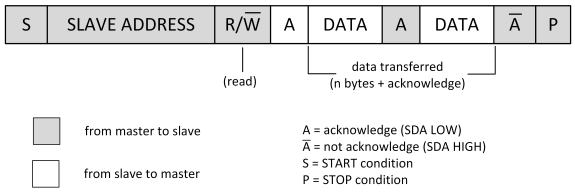

Figure 2.9: Data transfer from slave to master

The clock of the I^2C bus is set by the master. It determines the clock rate and therefore the speed mode of the bus . The clock rates are limited to their maximally permitted bus clock rate, but clearly distinguishable from each other. The following standardized bus speeds apply to the I^2C specification: [14]

- *Normal mode:* 100 kHz (100 kbit/sec)
- *Fast mode:* 400 kHz (400 kbit/sec)
- *Fast mode plus:* 1 MHz (1 Mbit/sec)
- *High speed mode:* 3.4 MHz (3.4 Mbit/sec)

2.2.1.2 Raspberry Pi as I²C-Master

This section describes how to configure a Raspberry Pi as master for the I²C and which software routines are needed. On Raspberry Pi 3, the I²C ports are located on Pin 3 (SDA) and Pin 5 (SCL) (see Figure 2.5). In order to be able to use the I²C, the interface in the kernel also needs to be activated. This can be done with Raspberry Pi configuration tool *sudo raspi-config/I2C-Enable*, Figure 2.10 shows the *raspi-config* setup.

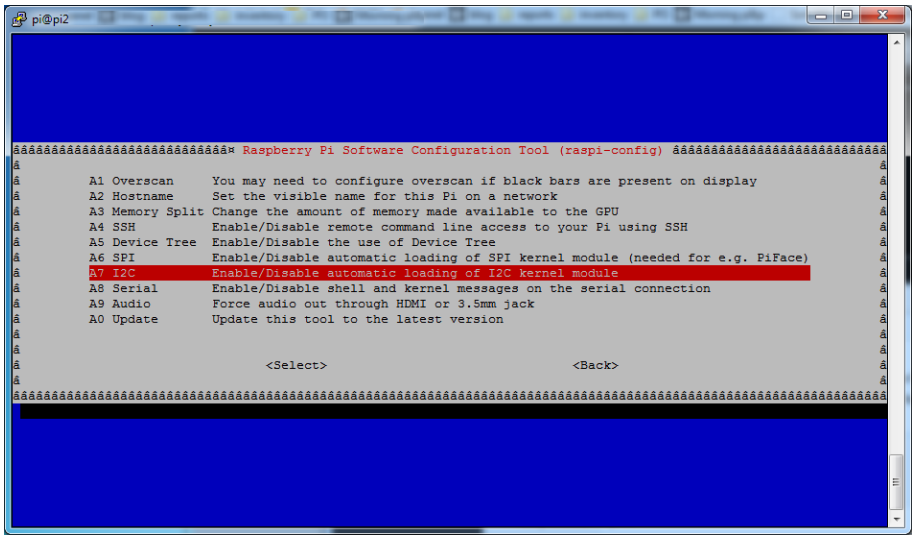

Figure 2.10: Raspberry Pi configuration tool

After the I²C interface at the Raspberry Pi is activated, it can be tested whether it is running or not. With the help of *i2cdetect -y 1* the serial bus is scanned for connected devices i.e. sensors or other ICs. The connected devices are listed in the figure below.

```
pi@raspberrypi $ sudo i2cdetect -y 1
0 1 2 3 4 5 6 7 8 9 a b c d e f
00: -- -- -- -- -- -- -- -- -- -- -- -- --
10: -- -- -- -- -- -- -- -- -- -- -- -- -- -- -- --
20: -- -- -- -- -- -- -- -- -- -- -- -- -- -- -- --
30: -- -- -- -- -- -- -- -- -- -- -- -- -- -- -- --
40: -- -- -- -- -- -- -- -- -- -- -- -- -- -- -- --
50: -- -- -- -- -- -- -- -- -- -- -- -- -- -- -- --
60: -- -- -- -- -- -- -- -- -- -- -- -- -- -- -- --
70: -- -- -- -- -- -- -- --
```

Figure 2.11: Raspberry Pi I²C bus scanl

For further details about I²C and the Raspberry Pi module, please refer to Configuring I²C reference guide. [1]

2.2.2 Red Pitaya

The Red Pitaya is an open source single board measurement device. This small measurement device offers the ability to replace the most commonly used measurements instruments such as oscilloscope, spectrum analyzer and signal generator. The data transfer is optionally possible via Micro USB, Gigabit Ethernet interface or WLAN-USB dongle. Figure 2.12 shows the Red Pitya with the available interfaces. [7]

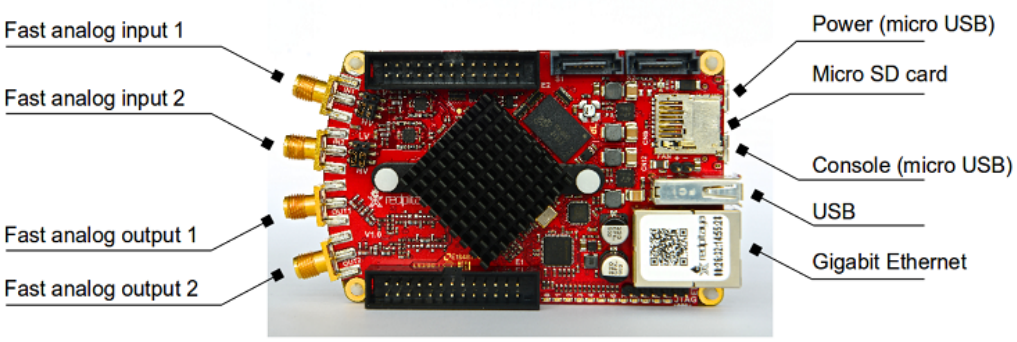

Figure 2.12: Red Pitaya board overview

The Red Pitay platform is based on the Xilinx Zynq 7010 SoC, which includes the FPGA block and the dual-core Cortex A9 processor. It runs on Linux operating system and can be controlled in various ways, some options include browser via PC or tablet, USB serial console or SSH protocol.

Crucial features for the application of Red Pitaya in this project is the oscilloscope and the function generator. It has two fast ADCs and two fast DACs, with a sampling rate of 125 MHz. The inputs and outputs have a resolution of 14 bit and a bandwidth of 50 MHz. The connection is made via two SMA connectors. In the table 2.1 are the specifications of the two analog inputs from the Red Pitaya.

Table 2.1: Analog input overview of Red Pitaya

Bandwidth	50 MHz
Sample rate	125 MS/s
ADC resolution	14-bits
Input impedance	1 M Ω
Default full scale input voltage	±20V
Input protection	Overload protection
Connector type	SMA

The table 2.2 shows the specifications of the two analog outputs of the Red Pitaya.

Table 2.2: Analog output overview of Red Pitaya

Sample rate	125 MS/s
DAC resolution	14-bits
Load impedance	50 Ω
Voltage range	±1V
Output slew rate	200 V/µs
Short circuit protection	YES
Connector type	SMA

In addition, the Red Pitaya is free programmable - in Python, C, Matlab, LabView and Scilab. Further information can be found in the user manual [21] of the manufacturer.

2.2.2.1 Standard Commands for Programmable Instrumentation (SCPI)

Standard Commands for Programmable Instruments (SCPI) was developed by merged companies whose members supported the standardization of the Interface language between computer and test instruments (measuring devices, voltage sources, frequency generators). SCPI was designed in the 1990s and also standardized as a part of the IEE 488. The SCIP command language is independent of the bus structure and can be transferred to the General Purpose Interface Bus (GPIB) or to the IEE 488, but also to the RS232-C, USB port, LAN Extensions for Instrumentation (LXI) or VXIBus. The SCPI commands can be created with every programming language (C, C++, Python, Java, etc.) and in every development environment. However, in order to issue commands and receive results, there must be an access from a programming language to a particular Bus system. SCPI commands are sent via ASCII Arrays in uppercase letters. To separate subgroups, a colon character is used (e.g. GEN: FREQ). With queries, a question mark character is added to the end of a command (e.g. GEN: FREQ?). Command line arguments of a particular command are added to the end of a command by the use of a space character. Numerical values are sent as a result of ASCII characters. If the command has more than one argument, they are separated by a comma character (e.g. ANALOG:PIN P10,1.8). In order to condense a command so that several commands are sent in one sentence, a semicolon character is added between the commands followed by a colon character (e.g. GEN:FREQ1000;:GEN:OFFSET 0,5). Another advantage of the ACII transmission is the transmission into a plain language so that any person can easily interpret the communication. In that way, the debugging is also significantly made easier. [6]

In order to control Red Pitaya Board with SCPI commands, initially the SCPI server needs to be installed on the Panel. The SCPI server receives the order through the TCP/IP protocol and appropriately interprets it. Red Pitaya can be controlled remotely over LAN or wireless interface using Matlab, Labview, Scilab or Phyton via Red Pitaya SCPI list of commands. Further information can be found in the user manual. [21]

2.2.3 Vector Network Analyzer

The Vector Network Analyzer (VNA) is an instrument used mostly in high frequency electronic devices which determines the measurements of the s–parameters but also reflection and transmission. For this purpose, the network analyzer transmitter sends a signal to the test object Device Under Test (DUT) with precisely determined frequency, amplitude and phase. It reflects a part of the signal and a further part passes through the DUT. The input signal is, as a rule, in its amplitude and phase changed. Figure 2.13 shows the basic operation of a VNA. [20]

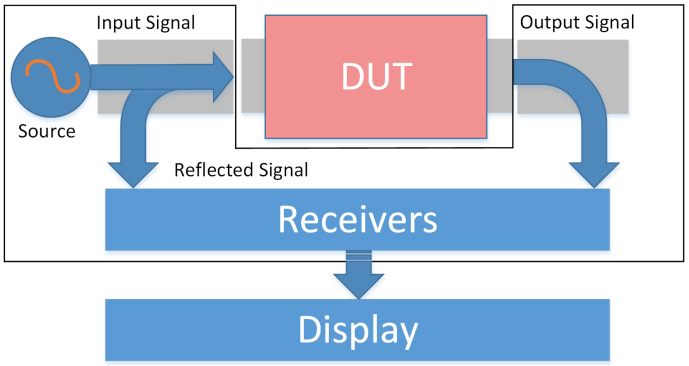

Figure 2.13: Basic block diagram of Vector Network Analyzer

From the measured signals (reflected input and output signals from DUT) VNA calculates the reflection (S11) as well as transmission (S21) and graphically represents these parameters on a screen as a frequency function.

Due to their sophistication properties, different network analyzers are utilized for laboratory and field operations. Furthermore, they differ by their frequency range which can certainly cover a reach from 5 KHz to 100 GHz as well as their transmission power and sensitivity but also their dynamic range. For automated measurements they can be equipped with different bus systems such as the General Purpose Interface Bus (GPIB), the LAN eXtensions for Instrumentation (LXI) or PCI eXtensions for Instrumentation (PXI). For data storage and documentation, they can have USB interface. [20]

2.2.3.1 miniVNA

In laboratory quality, the VNAs are very expensive and usually cost tens of thousands of dollars. Likewise, the market also offers different cost-effective solutions such as portable computer based VNAs. Such a device is a miniVNA (see Figure 2.14) made by mRS mini Radio Solutions which measures RFID antennas and RF circuits without any problems.

Figure 2.14: MiniVNA PRO- PC Based Network Analyzer

The miniVNA has two measuring ports to determine not only the return loss (S11), reflection coefficient (r), impedance (Z), VSWR (s) but also transfer characteristics of the network (S21) such as filters and HF bands.

Due to the calibration with an optional calibration kit (open, short, load,) the measurement results are precise and easily comprehensible. The impedance range (Z) varies from 1 to 1000 Ω, the dynamic range is up to 70 dB. The analyzer can be used as a low power HF generator as well. All processing, display and storage of data is done in the software on the host computer. The power supply is received via USB, thus external power supply is not necessary. Some of its features are summarized in Table 2.3. [13] [22]

Table 2.3: miniVNA PRO Specifications

Frequency Range	1 – 3000 MHz
Impedance Range (Z)	1 – 1000 Ω
Output Power	-6 dBm @ 500 MHz
Dynamic Range	90 dB in Transmission mode 50 dB in Reflection mode
Power Consumption	370 mA @ 5 V
System Type	2-port with S11 and S12
Weight	70 g
Dimensions	66 x 66 x 28 mm

2.2.3.2 miniVNA calibration for S11 measurement

The individual components of a network analyzer are containing errors, which means that they have a frequency and phase response. These so called system errors change the measured values, especially at higher frequencies so strongly that an exact statement about this can barely be made. Calibrating the analyzer leads to compensation of the system errors and the measurement accuracy greatly increase. For this purpose, successively different calibration standards with known electrical properties are connected to the test

ports and the measured values are determined. By calculating the measured values of the various calibration measurements, taking into account the known electrical properties of the standards, the error coefficients describing the system errors of the analyzer can be calculated.

The most important part, before starting with the measurement is the calibration of the miniVNA. Very often, the calibration method uses OPEN-SHORT-LOAD (see Figure 2.15) because it is suitable for reflection (S11) measurement. [22]

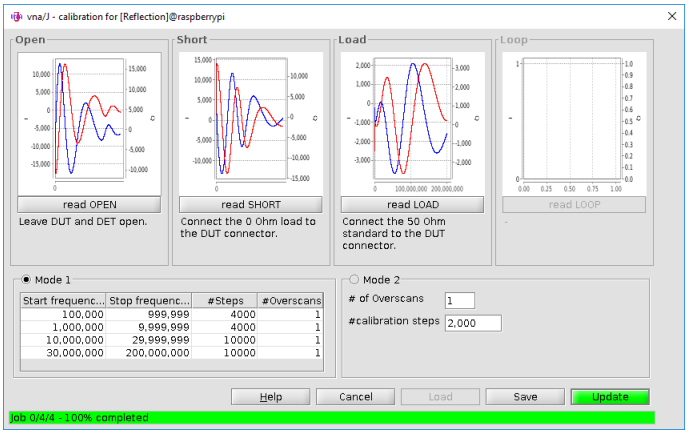

Figure 2.15: miniVNA PRO - Calibration Window

For the calibration could be used a calibration kit (OPEN-SHORT-LOAD), which is shown in Figure 2.16. In order to properly adjust the PCD an impedance measurement must be performed. The impedance measurement is an S11 measurement showing the normalized resistance and the reactance of the PCD antenna impedance in a Smith chart:

$$\underline{Z} = |\underline{Z}| \cdot e^{j\theta} = R + jX \tag{2.1}$$

$\underline{Z}$ ..... complex impedance
θ ..... phase between voltage and current
R ..... real part, resistance
X ..... imaginary part, reactance

Figure 2.16: MiniVNA PRO- Calibration kit

The Smith chart shows the normalized impedance. The most commonly used normalization impedance is 50 Ω. [3]

3 System Design

3.1 Requirements

As mentioned in the Chapter 1.2., in order to fulfill the prerequisites, a technical evaluation i.e. analysis of the TS is needed. In the first testing and validation step, the TS device was tested under laboratory conditions. During the analysis phase, the requirements and critical parameters by TS system were set.
There are three parameters as TS properties which might be critical for potential TS malfunction:

1. *Power supply (+12 V) for the relays*: Most errors can be detected with a Digital Multi Meter (DMM) by continuity tests, measuring voltage states or current consumption. In order to get a more accurate value for voltage and current, the Keithley 2400 Source Measure Unit (SMU) was used. Practical tests have shown that the current consumption is between 20 mA and 40 mA per measured relay.

2. *PCD reader antenna matching*: The PCD reader antenna matching shall be verified with the VNA. The VNA needs to be calibrated (open, short and load) before each measurement. The calibration should be done at an output power of 0 dBm. The target value for the PCD reader antenna impedance is 50 Ω +/-2 Ω tolerance.

3. *PICC module antenna resonance frequency*: The resonance frequency of the PICC module antenna is very difficult to measure. Many correlation measurements have been done and at the end the correlation parameter for the resonance frequency was defined in a form of a Vpp [V] induced voltage on the antenna pins, without the DUT. The Vpp [V] induced voltage on the antenna pins needs to be measured on each PICC antenna. Which voltage should be at the input of the PCD Reader antenna so that the certain induced voltage Vpp [V] can be measured was not the focus of this thesis. The measurement itself has to be done with the digital oscilloscope and passive probe with low capacitance.

In the table 3.1 the most important parameters are shown, along with the necessary measurement instruments to examine their functionality.

Table 3.1: TS most important parameters

TS components	Description	Measurement method
PCD	PCD reader antenna	VNA
PICC	PICC module antenna	Oscilloscope
Digital control	Control unit to switch the digital logic	DC check
Power supply (Relay)	Current and Voltage Monitoring	DMM
MDR Cable	Current and Voltage Monitoring	DC check
RF Cable	RF anlog signal cable	DC check

The test and evaluation results will be used to refine the requirements of the ADT. These test results will be presented in detail in the Chapter 4.1. After the requirements were defined, it was possible to proceed to the further development of ADT basic concept, which is presented in figure 3.1.

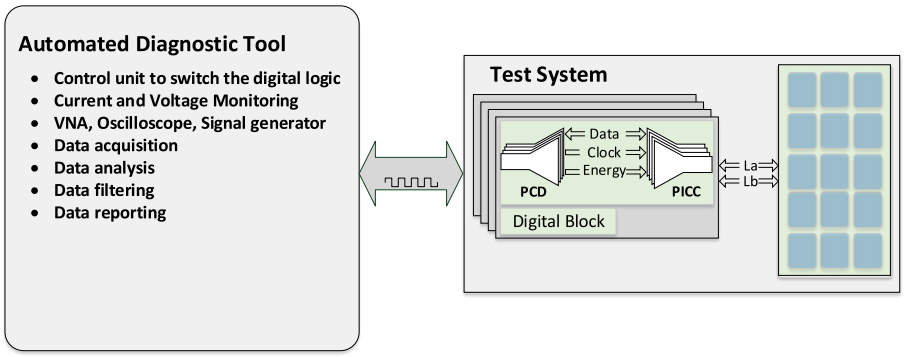

Figure 3.1: Basic overview of *Automated Diagnostic Tool (ADT)*

3.2 System Concept

This section of the master thesis deals with the exact requirements of the designed ADT, for which a prototype solution has to be developed and implemented. A requirement profile for the hardware-technical part of the ADT system was presented in the previous sections. These are the fundamentals for all further researches and decisions.

1. An essential feature of the ADT system must be that it is a standalone device.
2. The ADT system should be developed as modular as possible.
3. A single-board computer (Raspberry Pi) as a central control unit is recommended to ensure a high level of flexibility in advance.

4. I^2C bus is chosen for the communication between the modules and the single-board computer.
5. The ADT must be able to fully check the TS automatically. Therefore, it needs to be equipped with the following measuring instruments: oscilloscope, signal generator and VNA. Red Pitaya board was selected for the implementation of oscilloscope and signal generator. For the implementation of the VNA, the miniVNA board was selected.
6. In the domain of electronics, the most common standard components should be used to ensure the supply-chain of spare parts for the multi-year duration of the project.
7. A basic standalone software application (proof of concept) needs to be developed and integrated in the ADT system in order to configure its hardware system and to build a Graphical User Interface (GUI) application.
8. An enclosure prototype for new hardware components of the ADT needs to be designed and developed. A careful attention needs to be given when designing the front panel so that the ADT can be easy to handle.

The requirements from Chapter 1.1 and Chapter 3.1 defined the hardware concept, which are presented in Figure 3.2. Additionally the Software implementation and enclosure design on the ADT will be described.

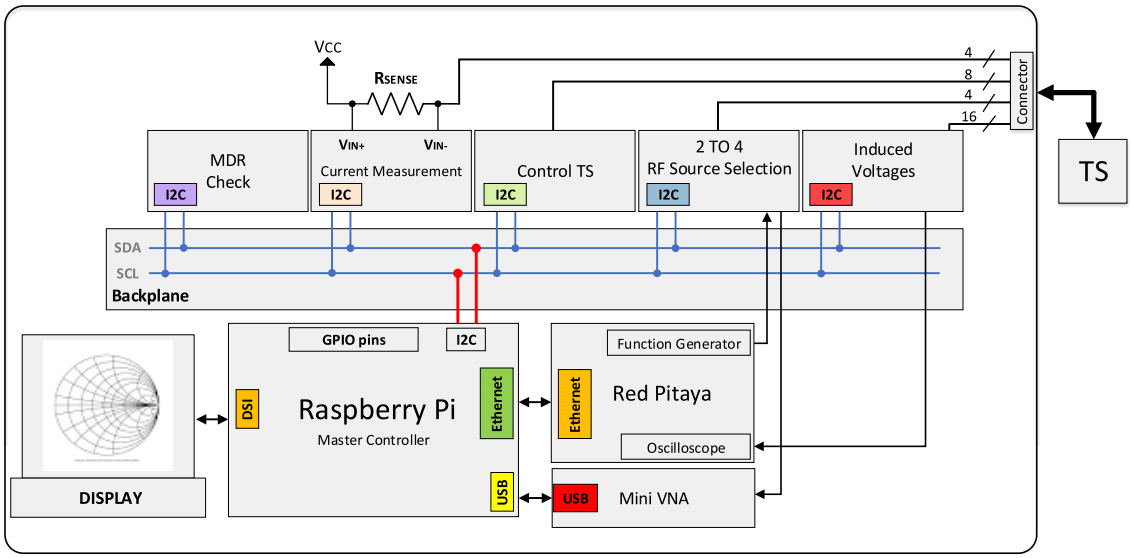

Figure 3.2: Overview of the complete concept *(ADT)*

3.2.1 Hardware Design

This chapter introduces the complete schematic design of the ADT system. For the realization of this project a modular system structure is used. A modular system consists of a backplane board, as well as various modules that are connected via connector (board to board). [4]

The main hardware system can be separated into five modules:

- Mini Delta Ribbon (MDR) Mainboard
- MDR Cabelcheck
- Radio Frequency (RF) selector
- Induced Voltage (IV) Mainboard
- Red Pitaya (RP) Adapter

The schematics were made in Altium Designer and complete schematics are listed in Appendix A.

3.2.1.1 Backplane Design

A backplane or backplane system is an electrical connector that connects multiple circuit boards together. The backplane connectors are parallel to each other so that each pin is connected to its corresponding pin and thus a complete system bus is put together. There are two types of backplane systems, an active backplane and a passive backplane. The active backplane holds the slots as well as the required circuitry in order to manage and control all the communication between the slots. On the other hand, a passive backplane is equipped only with the bus connectors and has little or no additional circuitry.

It was decided to use the passive backplane topology because the entire communication of modules is independent of each other. The connectors make a contact between the modules and the backplane. The connector for the modules should be capable of providing the modules with mechanical support in the ADT system. The selected connector is a modular high power and signal combo connector, it should provide sufficient support and be mechanically robust. Figure 3.6 shows the pin assignment of the EXTreme Ten60Power™ ET60S Series socket. [9]

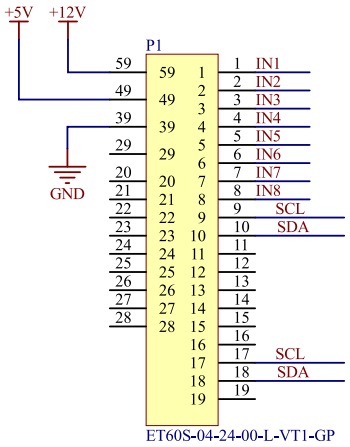

Figure 3.3: Pinout for ET60S Connector

The communication bus is made via the plug-in connectors as well as the required power supplies for the individual modules. The most important requisite for the backplane is that the communication bus should be equally available for all and be as simple as possible. The I^2C bus was selected as a common data bus. The bus only requires two lines for communication. More information about I^2C can be found in subsection 2.2. The backplane includes a common I^2C bus as well as power bus connected to an array of bus connectors. The power bus provides two power supply levels of 5 V and 12 V. The board is additionally equipped with seven ET60S socket connectors along with two status LEDs for the supply voltage. Red LED indicates the 12 V power supply and orange LED indicates the 5 V power supply. The complete schematic diagram of the circuit can be found in Appendix A.1.

Figure 3.4 presents the Printed Circuit Board (PCB) of the backplane. The PCB board is a two Layer PCB with the dimensions 280 mm x 180 mm.

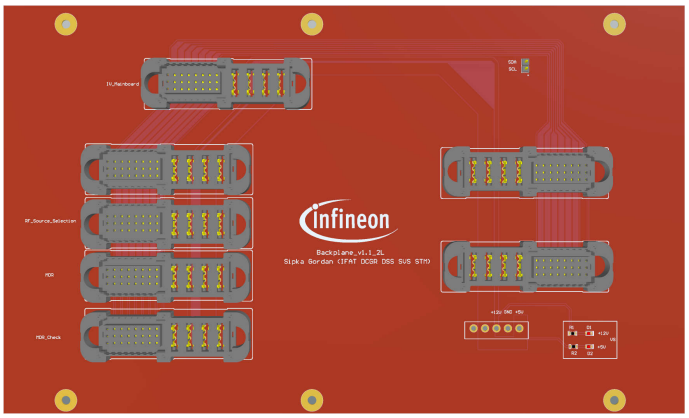

Figure 3.4: Backplane PCB- Top side of the board

3.2.1.2 MDR Mainboard

The task of the MDR mainboard is to generate digital test signals as well as to measure current and voltage. This enables the option to control the digital block of the TS and also to check all particular analog components for their functionality. See Figure 3.5 for the MDR mainboard block diagram.

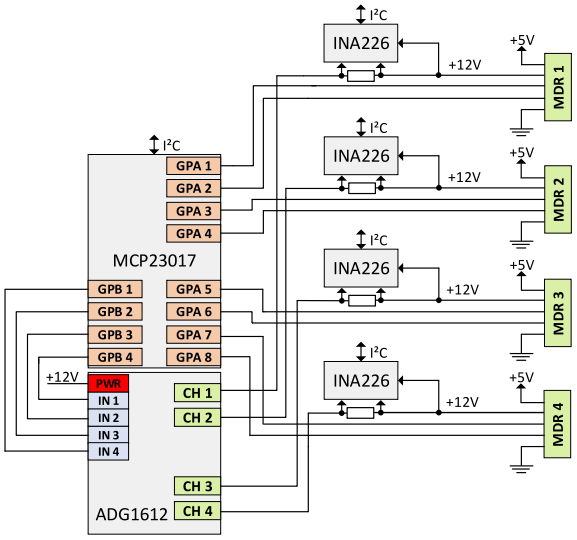

Figure 3.5: MDR mainboard block diagram

The connector provides the contact between the MDR mainboard and the backplane. Figure 3.6 illustrates the pinout of the connector that comes from EXTreme Ten60Power ™ ET60T series [8], which is a socket of the backplane circuit board.

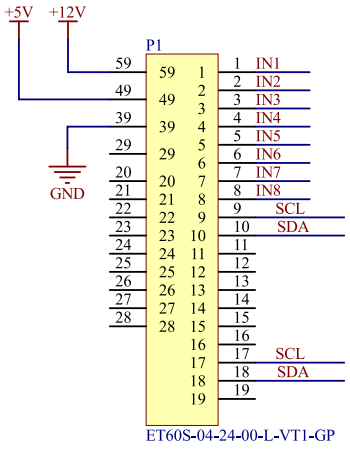

Figure 3.6: Pinout for ET60T Connector

Since the ADT uses a lot of digital GPIO for different functions (e.g. digital logic, status LEDs, Releys switching, ect.), it will be necessary to use additional GPIOs. The component

chosen for the port expander is the MCP23017 from Microchip Technology. The MCP23017 port expander has 2 ports (GPA and GPB) with 8 digital Input Output (IO) Pins each. In this case, 5 V supplies the chip, and that means output logic will be 5 V. The I^2C address is defined through the connections A0, A1 and A2, therefore a maximum of 8 expander components can be addressed. The SCL or SDA connections provide the access to the I^2C bus. Further information can be found in the data sheet. [18]

For the MDR mainboard module, three MCP23017 are integrated into the circuit, which means there will be 46 IO pins available.

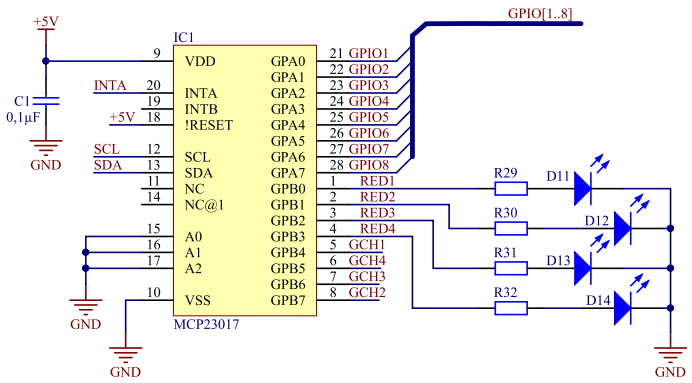

Figure 3.7: MCP23017 IC1 Application circuit

Since the IC1 is configured as an output, Port GPA is a control unit to switch the digital logic from a TS. Port GPB is used for the Status LEDs and Analog Switch (IC7), Figure 3.7 shows the wiring of these chips. The outputs on port GPA are also connected in series with the resettable fuse (Positive Temperature Coefficient (PTC)) in series with the IO pin, in combination with a Zener diode (see Figure 3.8). The PTC resistor limits the current flow through the Zener diode and lowers the overload between the applied voltage and 5V. Thus, the GPIOs are protected from the overload.

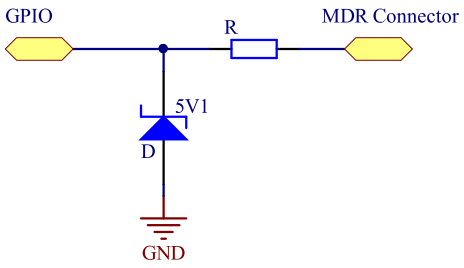

Figure 3.8: Overvoltage and overcurrent protection circuit

IC8 is wired for the purpose of monitoring the digital control signals. Some diagnostic lines from IC1 are connected to this Integrated Circuit (IC). By connecting these diagnostic lines from the port GPA to the IC1, an interrupt line from the IC1 to the host controller could be spared. Figure 3.9 shows the wiring of these chips. GPA is configured as an input and the port GPB is reserved for future use.

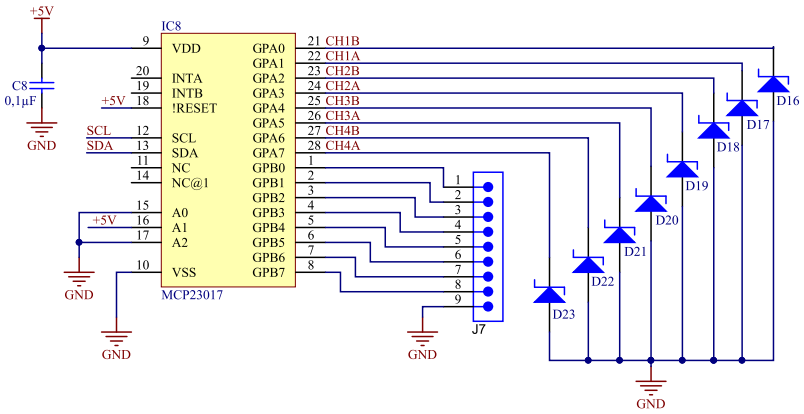

Figure 3.9: MCP23017 IC8 Application circuit

IC2 is used to connect freely programmable LEDs for status indication. The output ports of the MCP23017 provide an output voltage of 5 V and can be loaded with a maximum current of 25 mA. Figure 3.10 shows the wiring of these chips.

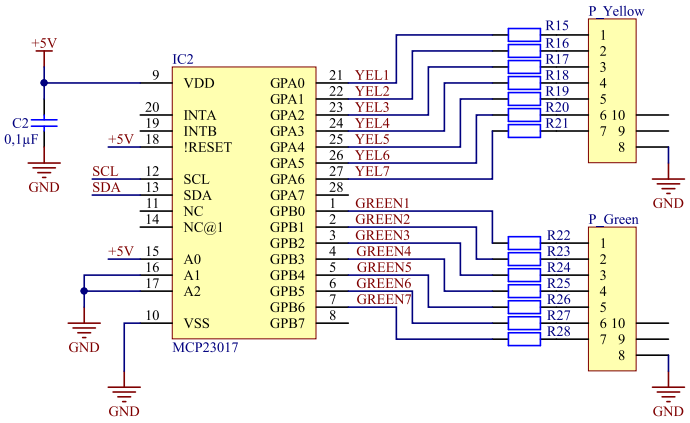

Figure 3.10: MCP23017 IC2 Application circuit

Figure 3.11 shows the wiring of an analog switch chip. This chip can be used to supply the individual analog components of the TS with 12 V range. For switching between four channels of the TS, a quad Single Pole Single Throw (SPST) switch will be required. The control of the analogue switch takes place via the port expander IC2. The model ADG1612BRUZ from Analog Devices was selected as analogue switches. Further information can be found in the data sheet. [2]

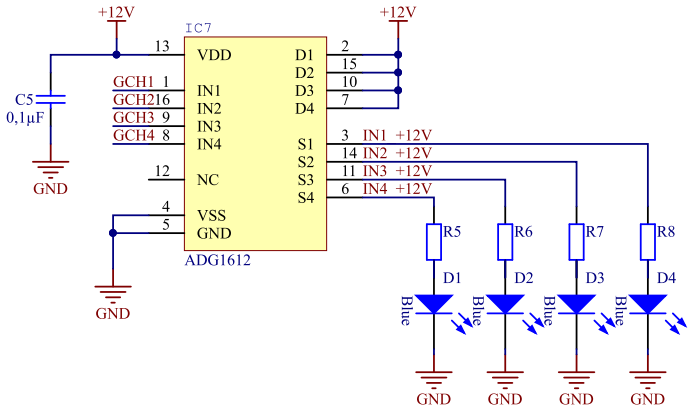

Figure 3.11: ADG1612BRUZ IC7 Application circuit

The current measurement is an important parameter for the realization of this project. It will be used to verify the current state of the TS, the current consumption on each relay of the TS will be monitored. A current sensing circuit is implemented on the ADT system as shown in Figure 3.5. The component chosen for current and voltage monitoring is the INA226 from the manufacturer Texas Instruments.

The INA226 is a current shunt and power monitor. INA226 calculates the current by measuring the voltage drop over a shunt resistor. The Current is calculated by multiplying the measured shunt voltage with a calibration value. The calibration value is the product of maximum expected current and the shunt resistor value. The input range of INA226 is ±82mV, so the size of the shunt resistor has to be carefully selected. It is also a device with an I^2C interface. Further information can be found in the data sheet. [15][18]

$$R_{shunt} = \frac{U_{shunt}}{I_{shunt}} = \frac{82\,mV}{I_{shunt}} \tag{3.1}$$

The maximum expected current in the system is 160 mA. The 500 mΩ can be used as shunt resistor. The complete application schematic of the INA226 is shown in Figure 3.12. An initial design for the MDR mainboard was created using five INA226s. Four INA226s are implemented to measure 12 V supply lines from each TS channel and one to measure 5 V supply line. The 5 V supply is used for voltage supply to the IC Decoder on the TS. This CMOS Decoder is used to decode the control signals.

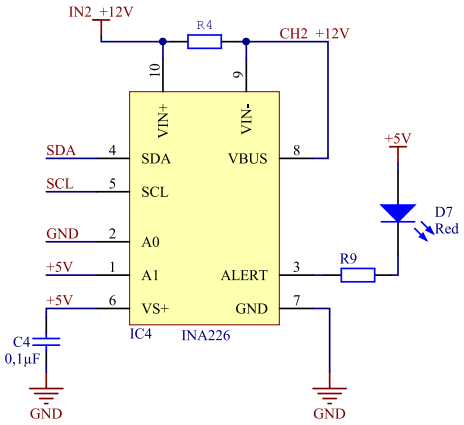

Figure 3.12: INA226 Application circuit

In order for the whole ADT system to be connected to TS, the connector will be the same as on the TS required. The MDR mainbaord is equipped with the four MDR connectors, in this case it is right angle connector. The connector pinout for MDR connector is show in Figure 3.13.

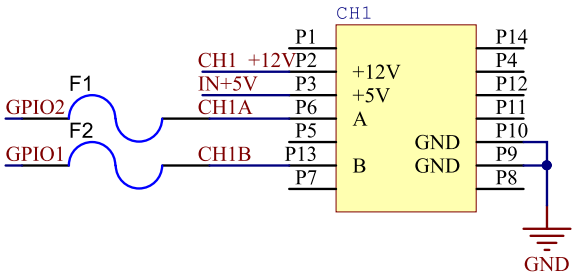

Figure 3.13: MDR connector pinout

The complete schematic diagram of the circuit can be found in Appendix A.2.

The MDR mainboard PCB layout was affected by several aspects of which the major ones will be discussed in this subsection. The first precondition was to determine the PCB dimensions. MDR Connectors have affected the dimension of this PCB. Four MDR connectors are used, dimensions 29.5 x 16.7 x 9.1 mm, and next to each connector there is a red status LED. In order for the entire system to be even simpler for use and to assembly, a space is left between each connector. The second precondition was to determine the PCB mounting routine. The concept itself is designed so that the MDR mainboard PCB is central, and that the PCB MDR cablecheck is mounted beneath it and with the PCB RF switch above it. To get the required dimensions, a pair of different cardboard model PCBs were made and based on this, it was possible to conclude that the size of this PCB is 200 x 130 mm.

Regarding the component placement itself, it is divided into 4 blocks symmetrically with MDR connectors. Which means that with each MDR connector there is an INA226 block along with its components but also overcurrent and overvoltage protection that is located

next to the connector. The port expander is positioned with the backplane connector, allowing for short wiring between the ICs and other components. In addition there are two status LEDs on the board, one for 5 V and the other for 12 V. Figure 3.14 presents the PCB of the MDR mainboard.

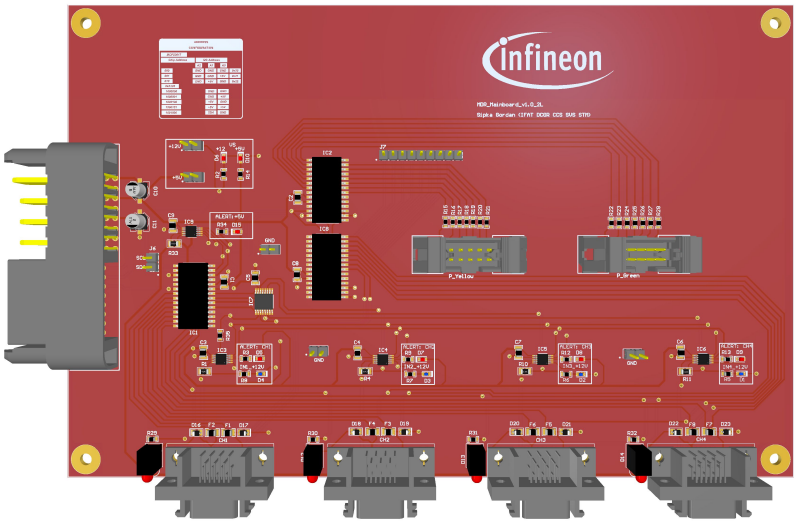

Figure 3.14: MDR Mainboard PCB - Top side of the board

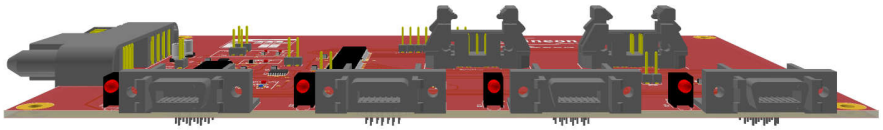

Figure 3.15: MDR Mainboard PCB - Front edge of the board

3.2.1.3 MDR Cabelcheck

The task of the MDR cablecheck is to be a tester of MDR cable. MDR cable is a connecting cable between RFID Reader and TS. It has a total of five wires that need to be tested. See Figure 3.16 for the MDR cabel check block diagram.

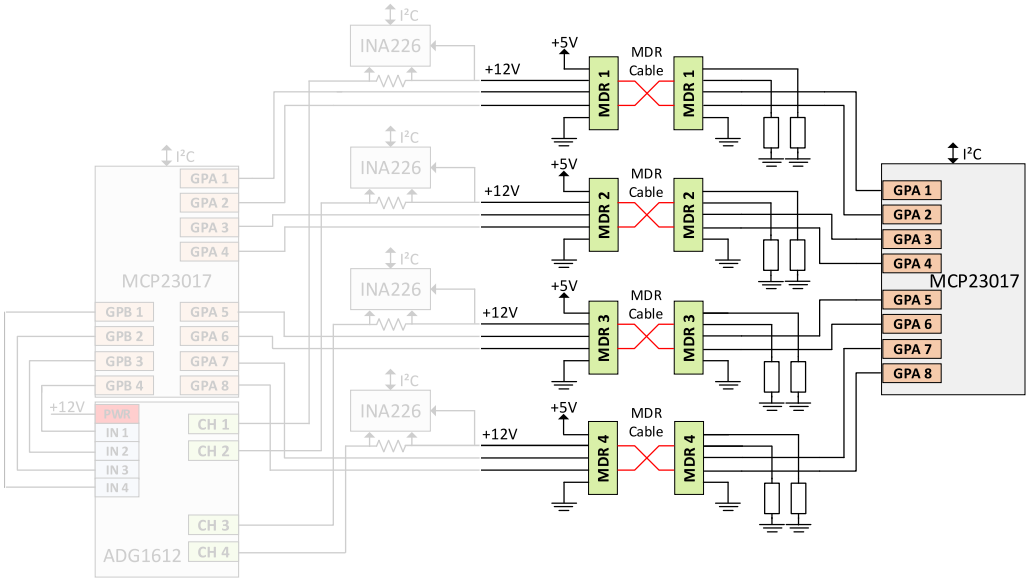

Figure 3.16: MDR cablecheck block diagram

A schematic described here is a simple tester that checks whether the MDR-cables are broken. The ET60T connector provides the contact between the MDR cablecheck and the backplane board. In this case, the IC1 port expander is responsible for the digital part and monitors the digital control signals. Figure 3.17 shows the wiring of these chips.

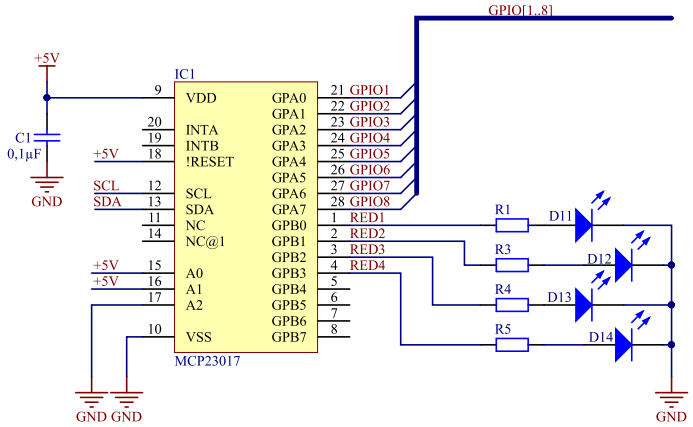

Figure 3.17: MCP23017 IC1 Application circuit

The IOs on port GPA are configured as input pins, therefore an overvoltage protection will be used. The output of the circuit is protected by a PTC and a Zener diode to avoid overcurrent and overvoltage. The IO port GPB are configured as output pins. They are used to connect freely programmable LEDs for status indication.

Other wires can be tested by monitoring the current and voltage that is implemented in the MDR Mainboard. For this part of the test procedure to work, additional resistors are added (see Figure 3.18). In this case, it will be High-side current sensing with resistance as load. The complete schematic diagram of the circuit can be found in Appendix A.3.

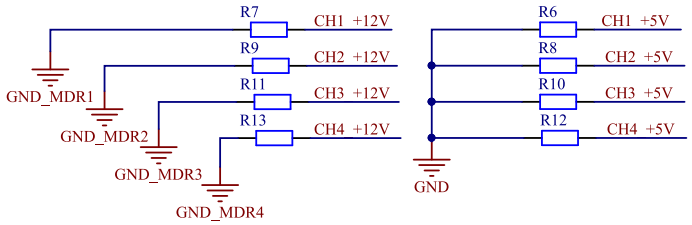

Figure 3.18: High-side current sensing, resistor as load

The physical dimensions of the PCB are given by the MDR Mainboard of the PCB dimensions. The component like MDR connector and backplane connector are placed in the same direction as the MDR mainboard. This will preserve the symmetry between these two PCBs, and the assembly itself will be simpler. In this PCB design only digital components are used and there is no need for splitting up in digital and analog ground. Figure 3.19 presents the PCB of the MDR cabel check.

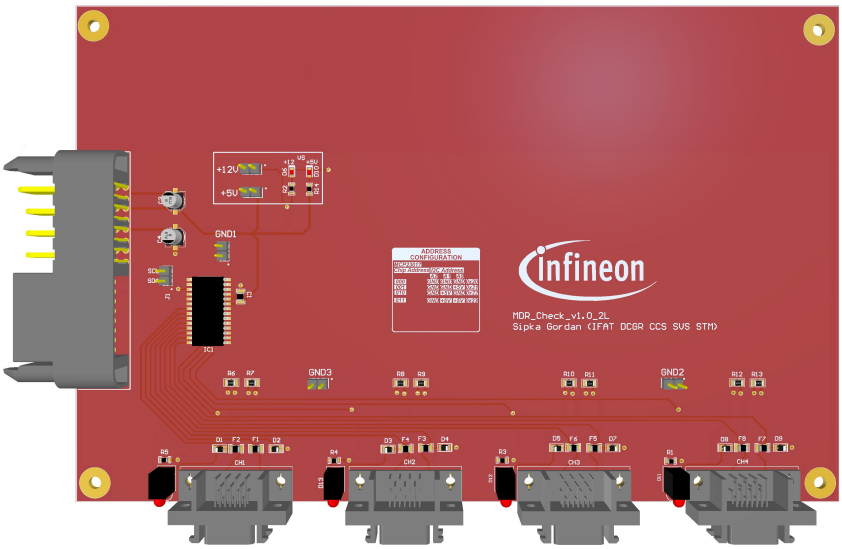

Figure 3.19: MDR cablecheck PCB- Top side of the board

3.2.1.4 RF selector

The task of RF selector is the multiplexing of analog signals. The multiplexer consists of two parts, an RF analog signal switch section and a DC switch section. The RF selector provides a path for the signal to Function Generator (FG) and from the miniVNA to the TS, while the DC switch produces the logic necessary to set the correct path in the RF selector. The RF selector also offers the ability to test RF cables, which means this is a multifunctional board with three input ports. Figure 3.20 shows how the multiplexer connects the miniVNA and FG to the TS system.

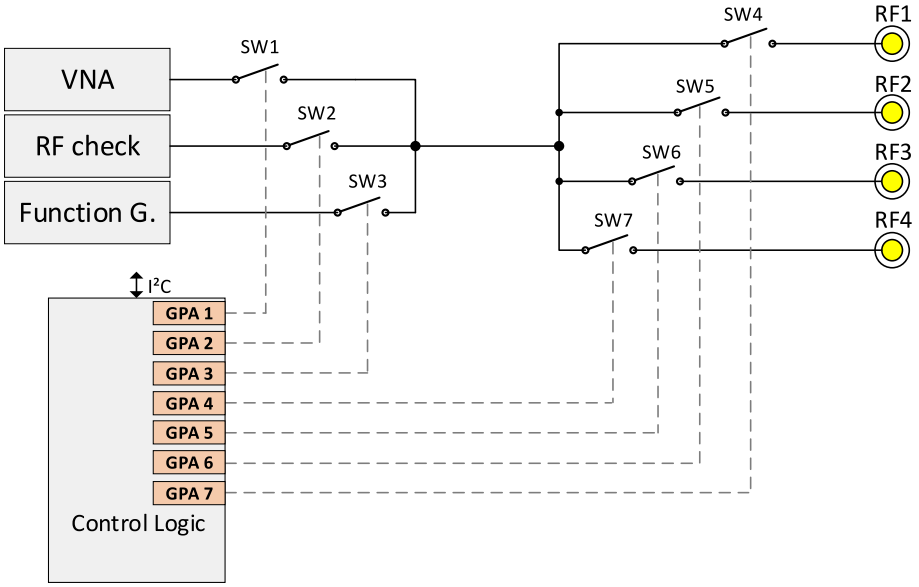

Figure 3.20: RF selector block diagram

An initial design for the RF multiplexer was created using 3 input ports to 8 output ports (these 8 ports are divided into 2 groups, each including 4 members). Since here is the case of analog signals that need to be switched, even during the conceptual phase, it was taken into consideration to design two topologies. One is a symmetrical design (where traces lengths are matched), another one is a non-symmetrical (where traces lengths are not matched). By its symmetrical and non-symmetrical design, the idea was to compare these two topologies. Topology with better performance will be used in further work, the TS itself needs only 4 ports. This section will be explained in detail in the chapter 4. The switches for analog signals used in this design are Reed Relay 9290-05 from Coto Technology, which are used for RF switching. The chosen 3:8 multiplexer switches operate in the frequency range of 10 - 20 MHz, a range that is needed for this project.

The ET60T connector provides the contact between the RF selector and the backplane board. IC1 is a port expander that is also used out of the need for more GPIOs and in this case the relays must be controlled (see Figure 3.21). The output current of the IC1 is too small for the relays, for this reason, additionally were used IC3 and IC4 (ULN2803). The ULN2803 device is a Darlington transistor array. The device exist of eight NPN Darlington pairs and the collector current rating of each Darlington pair is 500 mA.

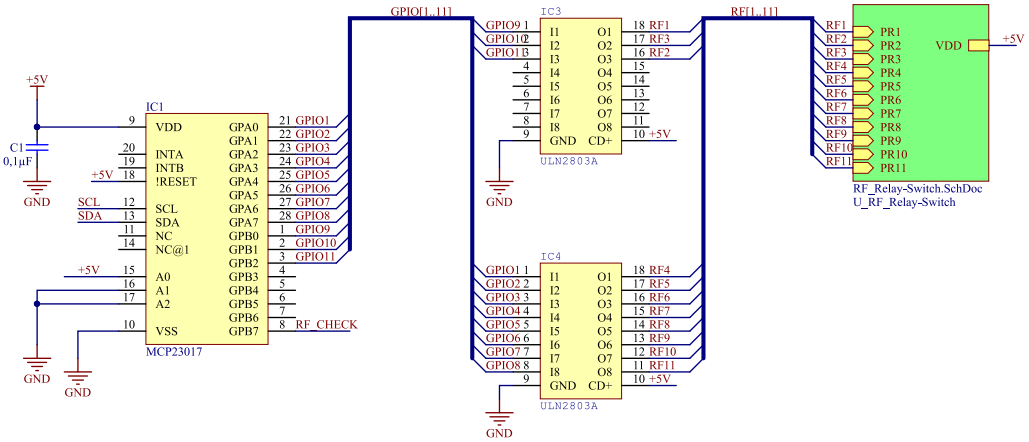

Figure 3.21: RF selector: Relay driver schematic

IC2 is used to connect freely programmable LEDs for status indication. Figure 3.22 shows the wiring of these chips.

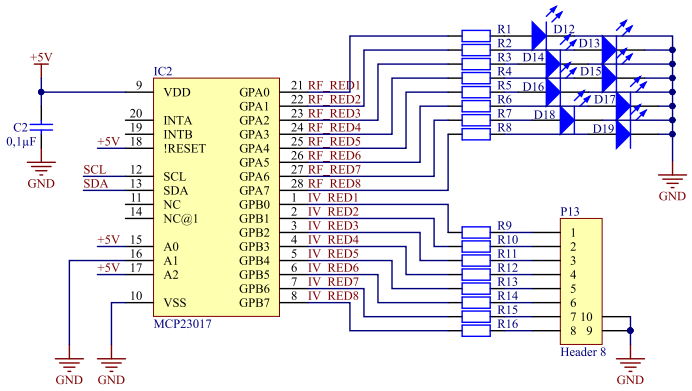

Figure 3.22: MCP23017 IC2 Application circuit

The complete schematic diagram of the circuit can be found in Appendix A.4.

This board used *coplanar waveguides with ground* for all of the RF traces and was designed that they are 50 Ω. These were obtained using the AppCAD impedance calculator for coplanar waveguide with ground. The figure 3.23 shows the calculated values.

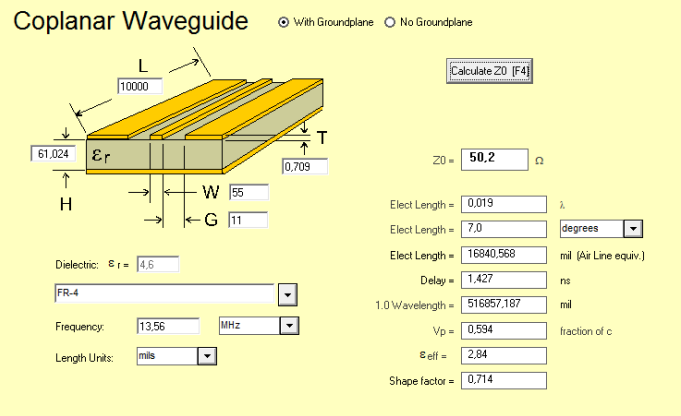

Figure 3.23: Properties of Coplanar Waveguide Calculation (AppCAD)

The top layer is used for routing the RF traces and the bottom layer is used for ground plane. The transmission lines have a grounded coplanar waveguide structure because it improves the shielding of the circuit against failure and reduces the unwanted crosstalk issue. This resulted in a trace width of 1.397 mm and a gap of 0.279 mm.

The final PCB design of the RF selector board is shown in Figure 3.4.

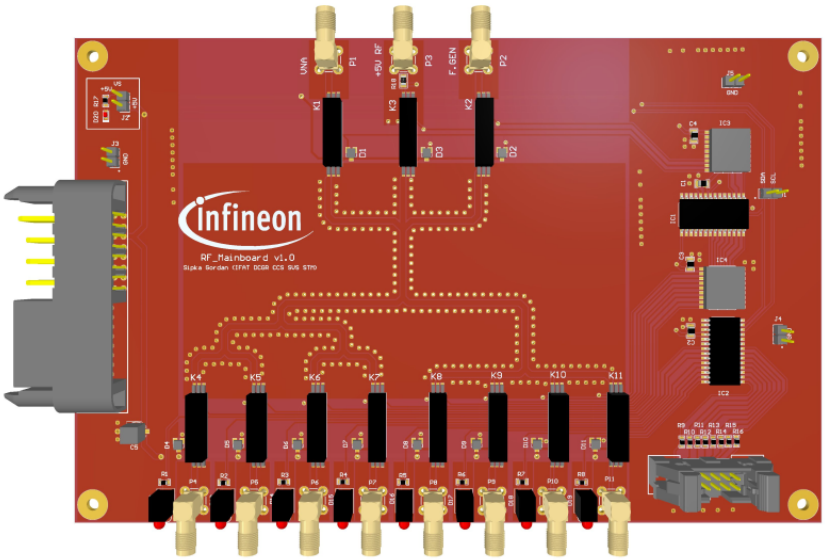

Figure 3.24: RF selector PCB- Top side of the board

3.2.1.5 IV Mainboard

The task of the IV mainboard is to enable the measurement of Vpp [V] induced voltage on each PICC antenna. The idea was to design a PCB that will be able to work as an oscilloscope probe. In this case, it is a passive probe. To be able to measure the Vpp [V] induced voltage on each PICC antenna board, it should have an analog signal 1:16 multiplexer. The Red Pitaya has the role of an oscilloscope, and its channel CH 1 is connected to the input from the IV mainboard to CH A. CH2 of Red Pitaya is also used for the analysis measurements. This channel is connected to CH B of IV Mainboard and serves to measure the crosstalk between the PICC antennas. The basics of the analog IV Mainboard are shown in the block diagram in the Figure 3.25.

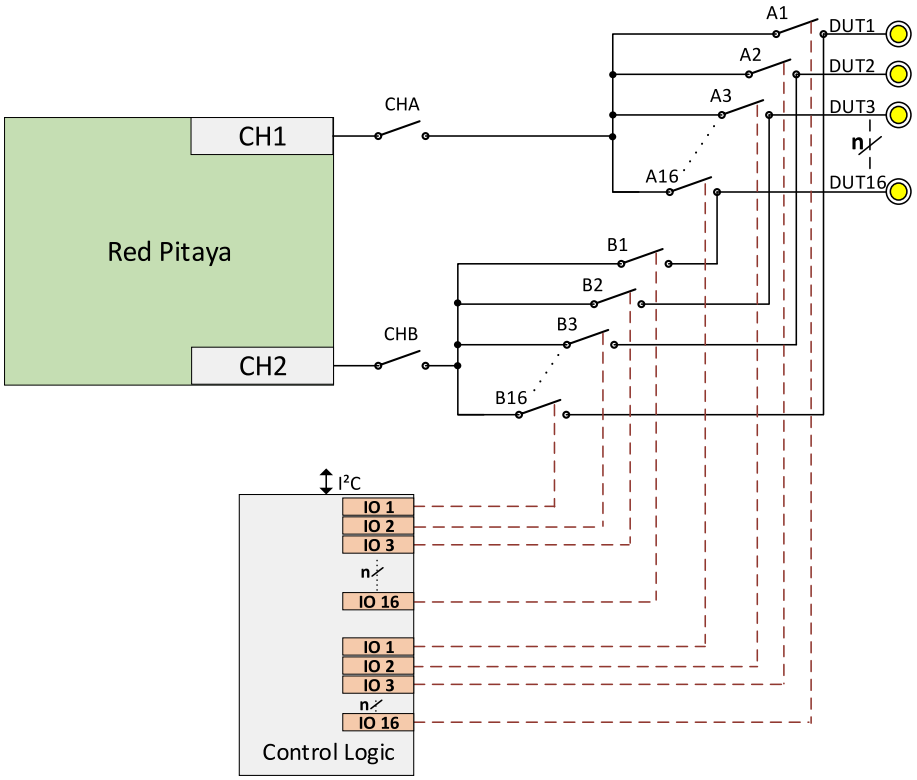

Figure 3.25: IV Mainboard block diagram

Both PCBs, including the previous PCB, need to be managed with a large number of IOs. In this case, it is about 32 IOs. In this case, the port expander MAX7312 from the company Maxim Integrated was used. Concerning functionality, it works like MCP2307. During the design process, a total of 5 such ICs were used.

This port expander also needs to control the individual relays, but there is not enough power on the output pins. For this reason, the ULN2803 IC1, IC3, IC4 and IC6 will be additionally used. Unlike the RF board where relays need 5 V for power supply, here the 12 V power supply is used. 12-volt power relays were selected to unburden a 5 V power bus. The switches for analog signals used in this design are Reed Relay

200-2-A-12-2D from PICKERING. The complete schematic diagram of the circuit can be found in Appendix A.7.

The IV mainboard PCB layout was affected by several aspects of which the major ones will be discussed in this subsection. The first precondition was to set the PCB topology and layout of the traces in a symmetrical way. All analog pairs of traces should be symmetrically routed. For the whole system to be symmetrical, the principle of circular design was used, which can be seen in Figure 3.26. For Circular design, a star topology was used, where one input is symmetrically distributed to 16 outputs. The same method was also implemented in the second block of this PCB. Thus, two circular blocks were made, with the intention of ADT to be compatible with all types of TS systems. The components within a controlling block were placed in the middle, close to each other with the main focus on minimizing the PCB trace length. At the same time, this was the most demanding part of designing PCB. The IV mainboard PCB is a multilayer PCB with six layers. These six layers make a routing of 32 relays. To help with debugging and giving visual confirmation of the system, LEDs are positioned at each relay indicating their status. Subsequently, it was possible to determine that the size of this PCB is 320 x 200 mm.

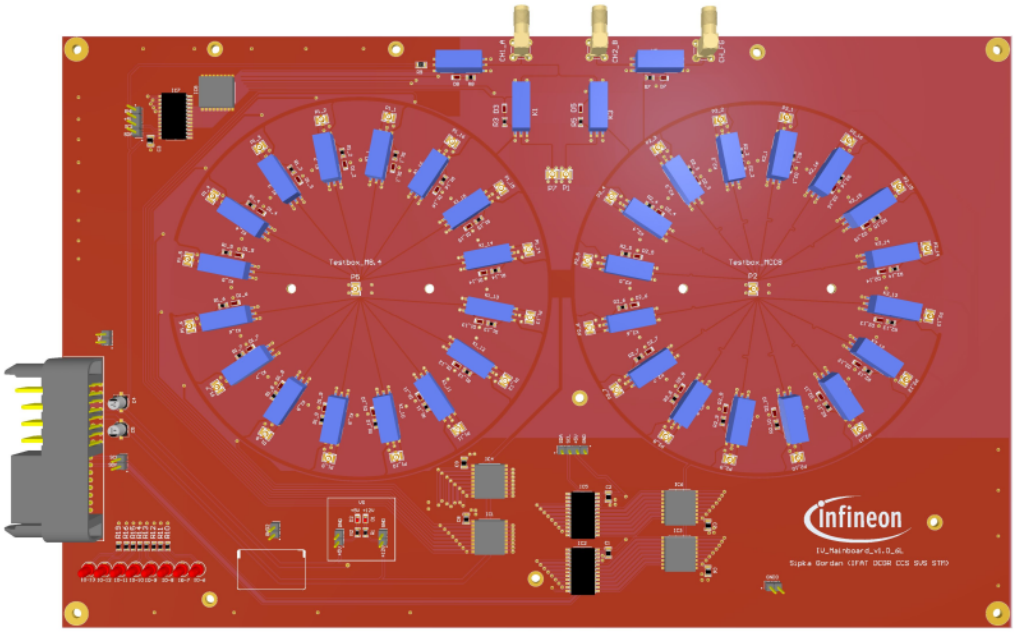

Figure 3.26: IV Mainboard PCB- Top side of the board

The second precondition was to determine the method of linking the star topology to the rest of the system. To ensure that the entire system remains symmetrical at the input/output of the star topology, it was necessary to use cable connector. For this reason, the UFL connector was used. By centralized approach, the Surface Mount UFL Connector is placed in the middle of the circle, which is connected with CH A or CH B. Using the same cables, each relay is connected to the PCB Adapter. These UFL series ultra-small coaxial cable assemblies are suitable for use in applications that require high frequency transmission using a small coaxial connector. This performance allows it to be used for the purpose of measuring the AC signal of 13.56 MHz. The Figure 3.27 shows the way how to connect the input/output from the IV mainboard with the use of the coaxial cable.

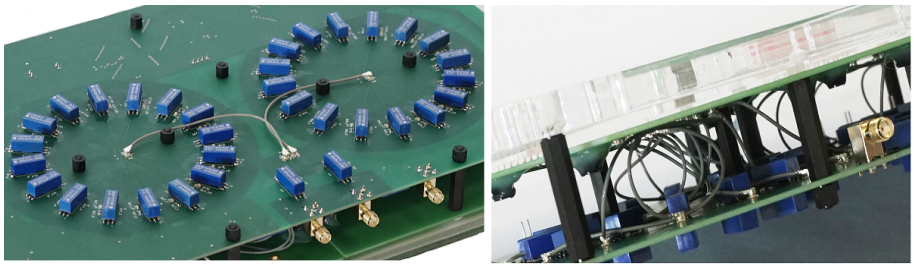

Figure 3.27: Coaxial cable connected input/output from the IV mainboard (left), Adapter board is mounted on IV Mainboard (right)

The third precondition was to determine the way to connect the IV mainboard to the TS system. For this reason, this PCB is mounted to the very edge of the backplane, so it is as close as possible to the top enclosure of ADT. In order to achieve such a physical contact between ADT and TS, an Adapter board with contact pads was additionally made, which can be seen in the Figure 3.28.

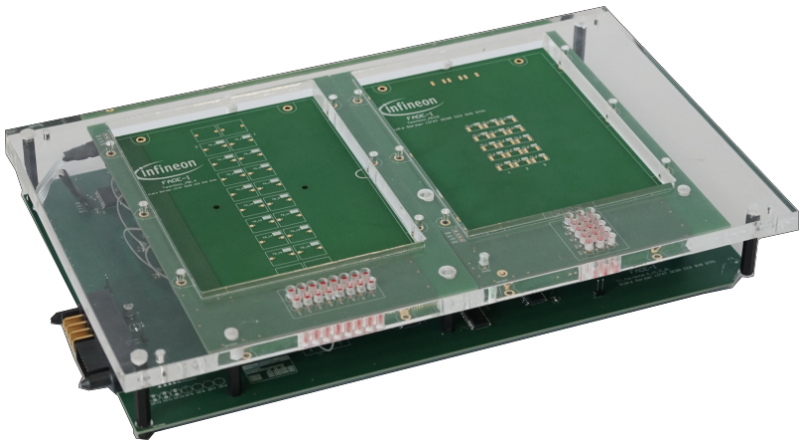

Figure 3.28: IV Mainboard with Adapter board

3.2.1.6 RP Adapter

The main task of the RP adapter is to provide power supply and communication of the bus interfaces with the other modules. See Figure 3.29 for the power supply and I²C bus implementation.

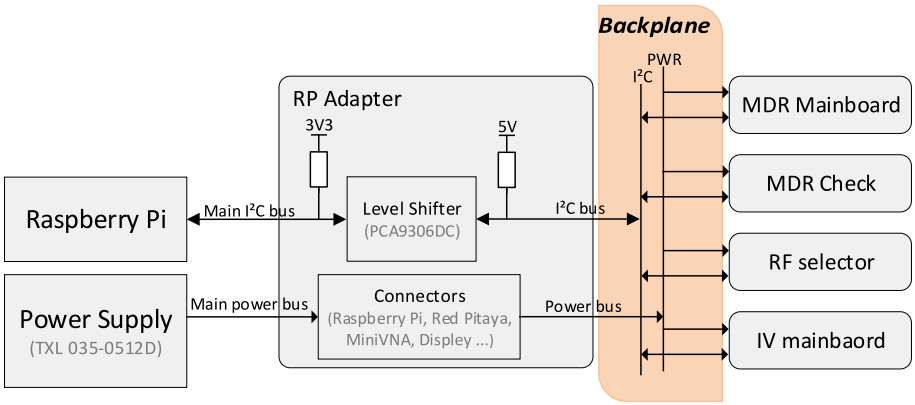

Figure 3.29: RP Adapter block diagram

The power for the system is supplied from the dual output TRACOPOWER TXL series power supply. A TXL 035-0512D is used as main DC supply, they provide power of 2.5 A at 12 V and 4 A at 5 V. This dual power supply is connected to the 5 pin Samtec IPBT-105-H1-T-S-RA-K power connector. The 5- pin connector is in addition connected to the fuses at 4 and 2 amps and was incorporated to serve as the first line of protection for PCB. Each supply line on the input stage is protected against voltage peaks by a unipolar TVS diode.

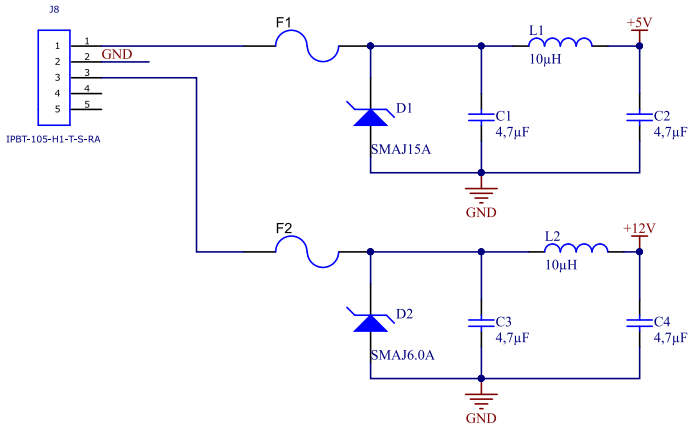

Figure 3.30: Power supply input lines for the fuses and LC filters

The ADT is controlled by a Raspberry Pi. The Raspberry Pi configures the ICs and gathers all the measurement data using the I²C interface. The Raspberry Pi is not assembled to the PCB, it is mounted to the Touchscreen, additionally fixed with screws on the corners. More details about assembly will be given later. The 40-pin ribbon cable is used

to connect the RP adapter to the Raspberry Pi. The communication bus is implemented using the PCA9306DC I^2C level shifter, because the Raspberry Pi I^2C Interface works with 3.3 V logic levels and is not with 5 V compatible. The I^2C signals from the Raspberry Pi with a voltage level of 3.3 V go through a level shifter to adjust the voltage level to 5 V. The schematic (see Figure 3.31) shows the pins on the connector for a Raspberry Pi and how the level shifter is implemented.

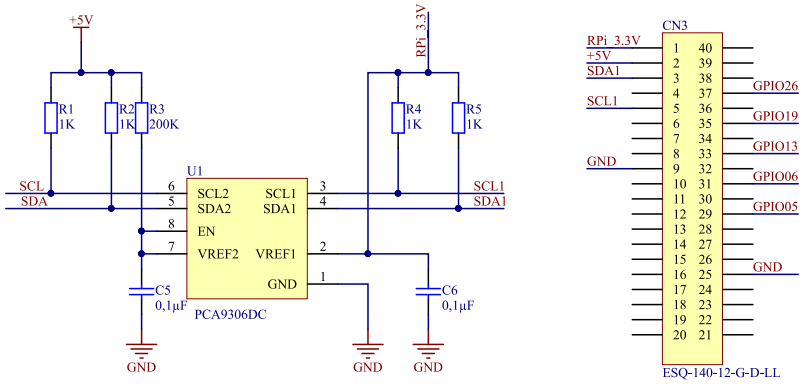

Figure 3.31: Raspberry Pi connector and level shifter

The complete schematic diagram of the circuit can be found in Appendix A.6.

Figure 3.32 presents the PCB of the RP Adapter. The PCB Board is a two layer PCB with dimensions of 280 mm x 180 mm. Red Pitaya is mounted on this PCB, which also affects its dimension. In addition to Red Pitaya, there are IDC Header for Raspberry Pi as well as a miniUSB connector for Touch Display power supply.

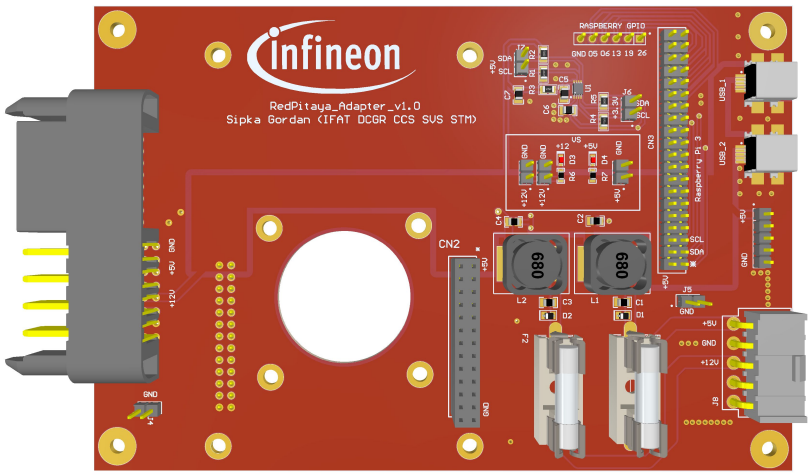

Figure 3.32: RP Adapter PCB- Top side of the board

3.2.2 Enclosure Design

This part deals with the development process of an enclosure for the ADT system, and with the goal to design a fully functional prototype. In order to make a good product, certain things must be known in advance about the matter. Firstly, the purpose of the product must be known, as well as its operating use case. There are also wide scope of rules and legislations regarding industrial equipment.[12][17] To find the required information about these topics, a pre-study was done with literature review and consultations with experts in the field.

The ADT enclosure needs a solution for making it possible to include different types of the Test System. A careful attention needs to be given when designing the front panel so that the ADT can be easy to handle. For the purpose of visualization and creation of manufacturing data, computer software DesignSpark Mechanical was used. This program allows importing PCB step file quickly and efficiently. Taking that into consideration, it is possible to represent the adequate enclosure. The PCB components which were developed in the Hardware phase are at the same time the prerequisite for enclosure dimensions. As soon as certain PCD modules are put in preferred order and once the adequate display is found, designing a front panel can begin (see Figure 3.33).

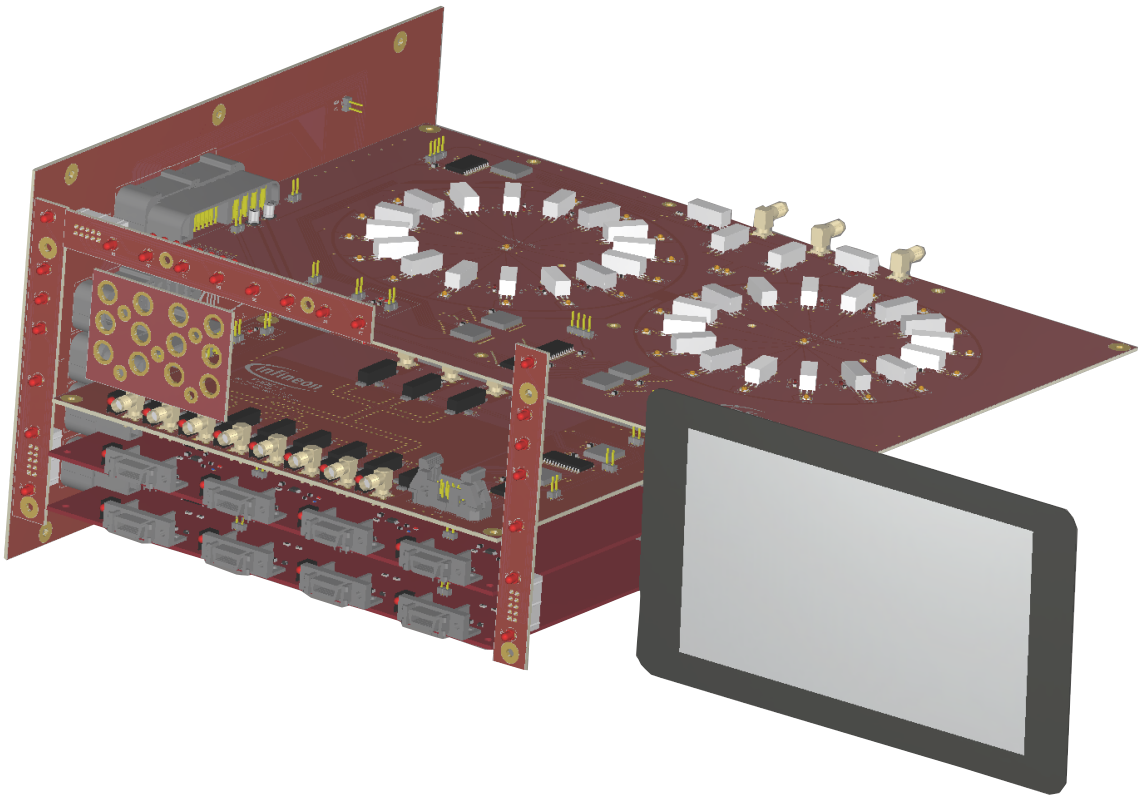

Figure 3.33: PCBs placement for the enclosure design

The final design was developed based on the conceptual idea of the front panel, as well as on the dimensions of the PCB module. The front panel has dimensions of 500 mm x 200 mm and the final front panel concept is presented in the Figure 3.34.

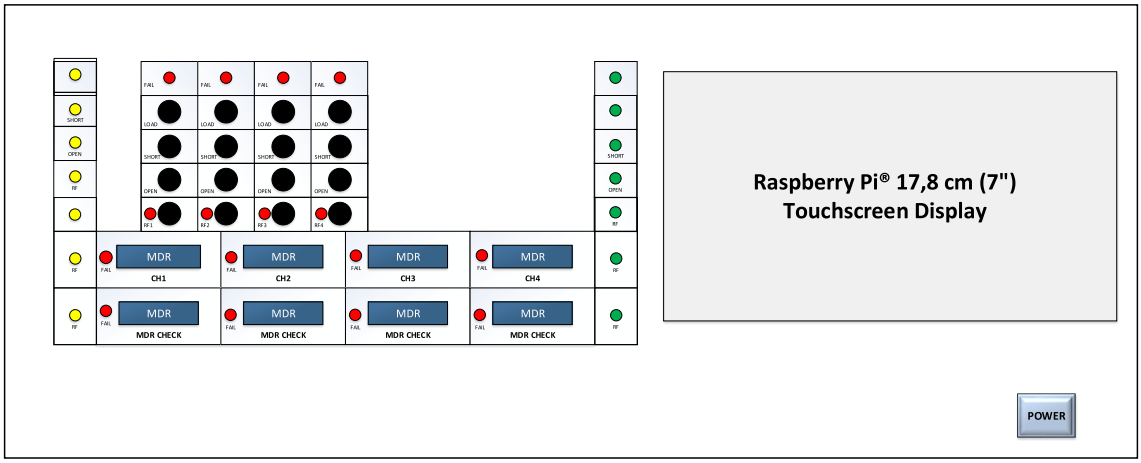

Figure 3.34: Overview of the front panel

In order to make the testing procedure of TS easier, LED lights were used as indicators and as a user guide. For this reason, different colors were used to distinguish different phases of the device testing. Yellow color signals the user to correctly connect the cables, green color signals PASS, while the red color signals FAIL. Such signalisation allows more practical visual control of the TS. Figure 3.35 shows the 3D view of the enclosure with the main body and it has dimensions of 500 mm x 200 mm x 350 mm.

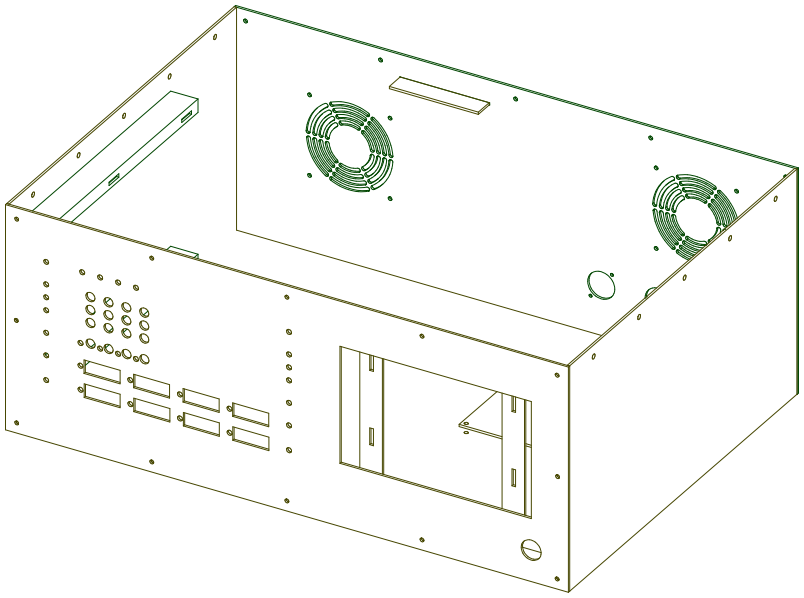

Figure 3.35: 3D View of Enclosure

Unlike the front panel and the rest of the enclosure, the top cover is made of Plexiglas. This was done to avoid the negative effects of metal on TS system. Figure 3.36 shows the final design of the ADT casing.

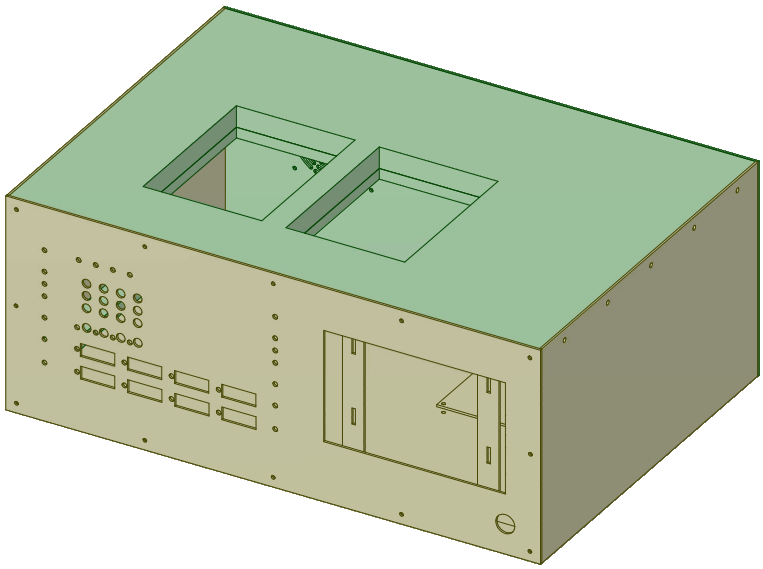

Figure 3.36: 3D View of Enclosure with top cover

After the enclosure design is completed, the next step is the formation of small mechanical components: calibration kit, LED adapter, display holder. Threaded bolts and buses are placed directly on the back side of the front panel so these components can be easily mounted. The Figure 3.37 shows all the additional components that were created to complete the ADT system.

Figure 3.37: Calibration kit with SMB adapter and LEDs adapter

3.2.2.1 Prototype Assembly

The prototype enclosure developed in phase (Enclosure Design) was produced in two units. Due to the low production volume, the assembly was performed by hand. A prototype of a complied ADT is shown in the Figure 3.38.

Figure 3.38: Prototype of the ADT

The TS is placed on the ADT and afterwards connected by MDR and RF cables, which is presented in the Figure 3.39.

Figure 3.39: Prototype of the ADT with connected TS

3.2.3 Software Design

This section describes the requirements and implementation of the software of the ADT. In subsection 3.1 and the subsection 3.2 the requirements of the ADT software are given. An interface (application) for Raspberry Pi was developed, to allow an I^2C connection which will be used in the communication to each modul. As well to allow Red Pitaya connection and to enable the control of the oscilloscope and the function generator, as well as to allow miniVNA connection with a basic function. Programming language used for Raspberry Pi is Python and the GUI was implemented with TKinter. See Section 2.2 to understand how to configure the Raspberry Pi. More details about Red Pitaya and the specifications of the miniVNA can be found in the same section.

For the ADT system software there are three main processes that the system requires to run. The first one is the initialization process, the second one is data acquisition and the last one is data reporting. The sequence of all these processes and procedures that run on the Raspberry Pi are shown in Figure 3.40.

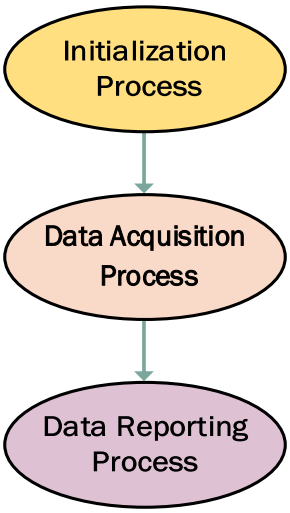

Figure 3.40: ADT main software flowchart

3.2.3.1 Initialization Process

This subsection will describe the initialization process of the ADT system. Initialization process is first step when the user starts the ADT application and there are three important steps that need to be taken before running it. See Figure 3.41 for the flowchart of the initialization process. The first step is I^2C bus scan procedure. This instruction is excuted using *smbus* routine. This will search I^2C for all ICs addresses, and after it will proceed to initialise the IO pins of the system and configure the current and voltage monitor. The next step is USB port scan procedure to check if miniVNA is properly connected to the Raspberry Pi. In this case the port name is */dev/ttyUSB0*. This instruction is executed

using *lsusb* routine. This is an additional package that needs to be installed onto the Raspberry Pi.

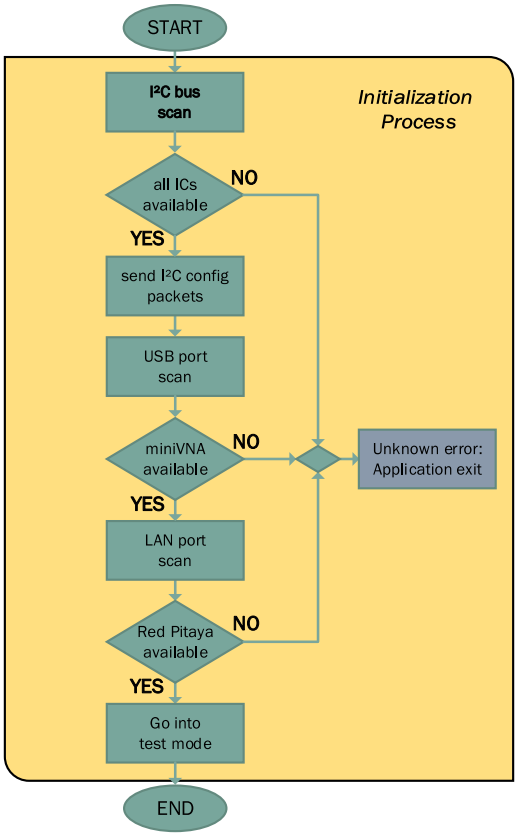

Figure 3.41: Initialization process test flow

The last step in initialization procedure is to check whether the Red Pitaya is properly connected to the Raspberry Pi. This instruction is executed using *redpitaya_scpi.py* script. This is the standard script to establish the connection between Raspberry Pi and Red Pitaya board. For more information regarding the remote control Red Pitaya can be found in the user manual.

Probably the most important item for the ADT software is the initialization process routine. ADT system hardware is designed in that way that the device has the possibility to perform the self-check as well as to control and examine the larger part of its most important parts or blocks. For example, it can test the power bus, communication bus, control bus, etc. with the goal to minimize its error while testing the TS. On the following page, the examples of how the implementation of certain registers, both on port expander and on current and voltage monitor, is presented.

After the complete initialization procedure is performed, the ADT system is ready for the next state (data acquisition), which means that the ADT is ready for Test Procedure of the TS.

The code snippet below is only a small piece of the script for I2C configuration routine.

```
#    I2C ADDRESS/BITS
#---- MDR-Mainboard
YeGr_LED = 0x21
MDR_Control = 0x20
MDR_Check = 0x22
MCP_ADDRESS = [0x20 ,0x21,0x22,0x23]  # Device Address MCP23017
INA_ADDRESS = [0x40,0x44,0x41,0x45,0x48] # Device Address INA226
#---- MDR-Check
MDR_Cable_Check = 0x23
#    IO-Expander Registers MCP
MCP_REGISTERS = [0x00,0x01,0x14,0x15] # Device Registers MCP23017
IODIRA = 0x00
IODIRB = 0x01
GPIOA = 0x12
GPIOB = 0x13
OLATA = 0x14
OLATB = 0x15
```

The code snippet below is only a small piece of the script for port expander configuration routine.

```
def InitADT():
    #print ("Start initialization...")
    IoOutAdrs = [RF_LEDs,YeGr_LED,MDR_Control,IV_AdA,IV_AdB]
    IoInAdrs = [MDR_Check,MDR_Cable_Check]
    IoLats = [OLATA,OLATB]
    IoDirs = [IODIRA,IODIRB]
    IoOutMAXAdrs = [IV_AdapTS_A,IV_AdapTS_B,IV_Cont]
    IoMAXLats = [Port1Config,Port2Config]
    IoMAXDirs = [OutPort1,OutPort2]
   #RF_switch
    bus.write_byte_data(RF_Rel, IODIRA, 0x00)
    bus.write_byte_data(RF_Rel, IODIRA, 0x80) #RF-Check as input
    bus.write_byte_data(RF_Rel, OLATA, 0x00)
    bus.write_byte_data(RF_Rel, OLATB, 0x00)
```

The code snippet below is only a small piece of the script how to configure the current and voltage monitor.

```
def InitADT():
    #print ("Start initialization...")
for ina_device in INA_ADDRESS:
        for ina_register in INA_REGISTERS:
            if ina_device == 0x48 and ina_register == 0x05:
                #=====================================================
                bus.write_word_data(ina_device,ina_register,0x002)#
                    Calibration Register 05h -> 0x200
                time.sleep(0.1)
            else:
                #=====================================================
                bus.write_word_data(ina_device,ina_register,0x004) #
                    Calibration Register 05h -> 0x400
                time.sleep(0.1)
```

3.2.3.2 Data Acquisition

This subsection describes the ADT data acquisition routine. The software development part includes customization and integration of all functions, based on the defined measurement processes and requirements. Regarding the structural hardware modules of the ADT system, four main software blocks need to be implemented: control unit, voltage and current monitoring, impedance matching and measurement of induced voltage. Inside each block there are several sub-blocks (e.g. easy functions for the control: LED lights, relays, ect.) which are linked together and allow the communication within the main blocks.

Figure 3.42 shows the standard test procedure, which was implemented. The initial test procedure was to check MDR cables, next the RF cables and later to check TS (see left Figure). However, the customer feedback is that this method is not optimal, due to disconnecting the cables from TS in order to preform the cable check (see right Figure).

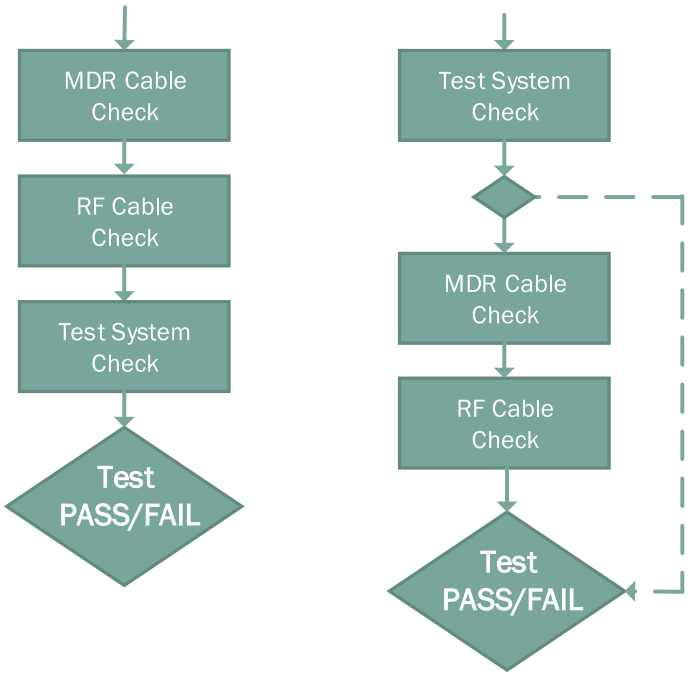

Figure 3.42: Test flow with standard test procedure

For this reason, the change of the test procedure is in place by first checking the TS. In case the test report is FAIL, first MDR cable is tested, followed by RF cable.

Figure 3.43 shows a simplified flowchart of the main modules which constitute the data acquisition processing.

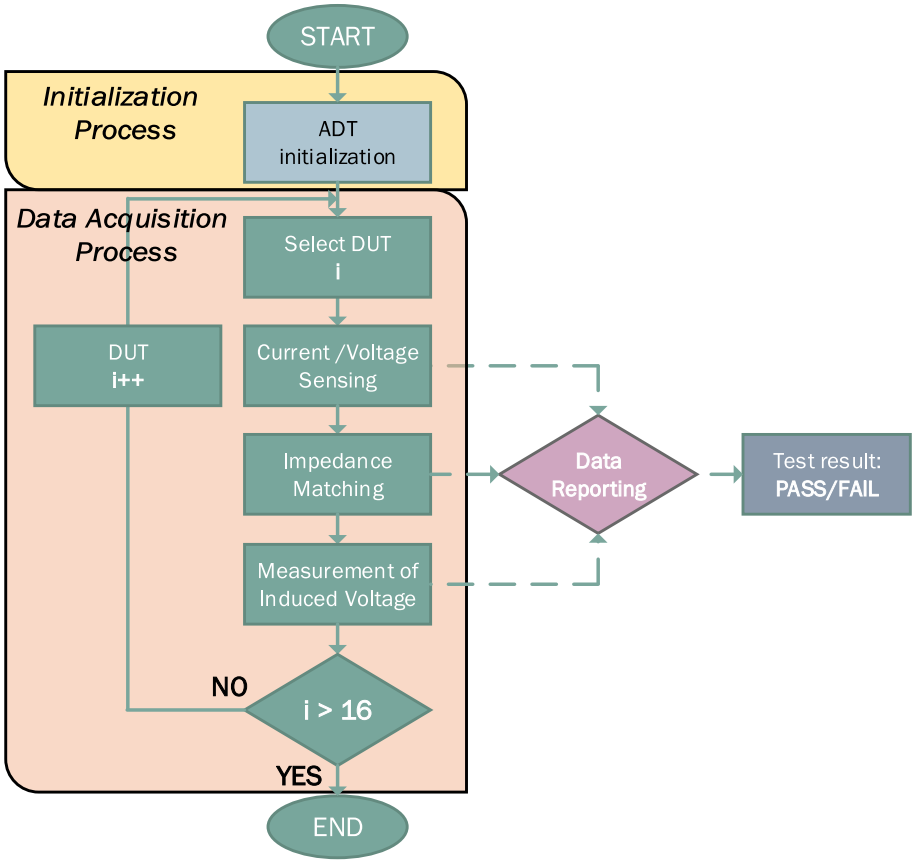

Figure 3.43: Data acquisition test flow

For this purpose a set of Python functions as well as scripts have been programmed. The function names and their description are mentioned bellow.

- *enableTG:* Function for control unit to switch the digital logic of TS.
- *getCurrent(TGNr):* Function for Current monitor.
- *getVoltage(TGNr):* Function for Voltage monitor.
- *TestSystemCheckDC(LogFileName):* Script for DC check of the TS.
- *checkTSCable(TSNr):* Script for MDR cable check.
- *RFCableCheckDC(LogFileName):* Script for RF cable check.
- *IVSourceChannel(TBType):* Function for induced voltage control.
- *Oscilloscope ():* Function for RP Oscilloscope control.
- *FunkGenerator(amplitude,waveform,frequency):* Function for RP Function Generator control.

The code snippet below is only a small piece of the script for control unit to switch the digital logic of TS.

```
def enableTG(TGNr):
    if TGNr < 0 or TGNr >= 5:
        return False
    TgAd = TG_ADDRESS[TGNr-1]
    bus.write_byte_data(MDR_Control,OLATB,TgAd)
    time.sleep(0.5)
    Current = getCurrent(TGNr)  #INA-address depends on TGNr
    if Current > 160:     #check if Overcurrent occu
        bus.write_byte_data(MDR_Control,OLATB,0x0F) # Disable 12V and set
            all red LEDs
        print("Over Current")
        return False
    Voltage = getVoltage(TGNr)  #INA-address depends on TGNr
    if Voltage < 11:     #check if Voltage is ok
        bus.write_byte_data(MDR_Control,OLATB,0x0F) # Disable 12V and set
            all red LEDs
        print("Under Voltage")
        return False
    return True
```

The code snippet below is only a small piece of the function for Voltage monitor.

```
def getVoltage(TGNr):
    if TGNr < 0 or TGNr >= 5:
        return False
    InaAdr = INA_ADDRESS[TGNr-1]
    result = bus.read_word_data(InaAdr, 0x02)
    getVal = ((result<<8) | (result>>8)) & 0xFFFF    #Byte Swapping
    BusVoltage = getVal*0.00125
    return BusVoltage
```

The code snippet below is only a small piece of the function for Current monitor.

```
def getCurrent(TGNr):
    if TGNr < 0 or TGNr >= 5:
        return False
    InaAdr = INA_ADDRESS[TGNr-1]
    result = bus.read_word_data(InaAdr, 0x04)
    getValue = ((result<<8) | (result>>8)) & 0xFFFF #Byte Swapping
    Current= getValue *0.01
    return Current
```

3.2.3.3 Data Reporting

In this subsection the routine of software implementation for data reporting in the ADT system will be described. So far, the ADT application for the automatic check of the TS has been implemented using the Python script and the next step is to create a script where the measured data will be stored. Data Reporting process is the step when the user starts the measurement procedure of the ADT application, which consists of three separate phases. See Figure 3.44 for the flowchart of the data reporting.

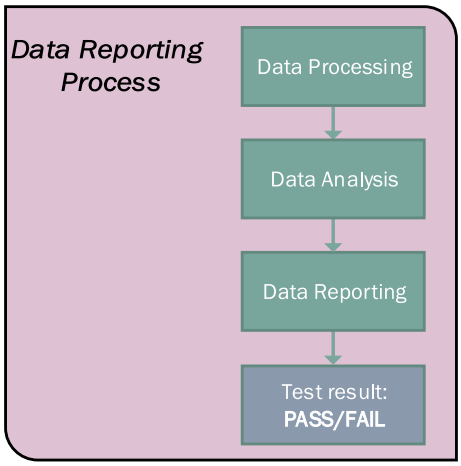

Figure 3.44: Data reporting test flow

The first phase (Data Processing) of the measured values begins with averaging the values and comparing them with internal limits (e.g. comparison with the minimum and maximum expected values) and as such will be used to shift to the next stage (Data Analysis) where it will be determined whether these values are PASS or FAIL. After that, the measured data enters the third phase (Data Reporting), where all data is specifically logged (in a .dlog file). In addition, a test report containing user related information is created. After completion of the TS measurement, the result (PASS or FAIL) is output.

3.2.3.4 Graphical User Interface

The goal of this subsection focuses on creating a simple and highly flexible GUI application (proof of concept) that allows easy implementation of all developed processes (as described in previous section). Python platform has available several software packages for the creation of a GUI, one of them is the Tkinter used in this application. Tkinter is an open source, portable graphical library designed for use in Python scripts.

To be able to use the GUI Widgets (e.g. Button, Checkbutton, Label, Radiobutton, etc.), Tkinter must be imported at the beginning of the software. The code snippet below is a main part of the Python code that enables the full functionality of their GUI tool.

```
from tkinter import *
from tkinter import messagebox
from tkinter import filedialog
import _thread
import time
import smbus
from ADT_config import *
from I2Cconfig import *
from meas import *
import shutil
import datetime
DemoMode = 0

class App:
        def __init__(self, master):
        # Init Command Button function
        def InitFade(self):
        # MDR Cable Check Command Button function
        def MDRCC(self):
        # RF Cable Check Command Button function
        def RFCC(self):
        # Testbox Check Command Button function
        def TBC(self):
root = Tk()
root.title("ADT: V0.1a")
root.geometry("800x480")
IFXlogo = PhotoImage(file="./bin/logo-desktop-en.gif")
Fadelogo = PhotoImage(file="./bin/ADT_logo.gif")
CapType = IntVar()
TbType = IntVar()
OperatorListStr = StringVar()
TestBoxStr = StringVar()
app = App(root)
root.mainloop()
root.destroy() # optional; see description below from Tkinter import *
```

All main blocks or functions are defined in the *App* class. The most relevant functions within of this class are mentioned bellow:

- *def InitFade(self):* initialization Command Button function
- *def MDRCC(self):* MDR Cable Check Command Button function

- *def RFCC(self):* RF Cable Check Command Button function
- *def TBC(self):* Test system Check Command Button function

There is a step-by-step function called procedure, dependent on the previous defined User test procedure. Moreover the produced GUI will be useful in generating the test report that enables saving the output results as a text file. Figure 3.45 shows the GUI when the initialization phase for the ADT devices has been performed.

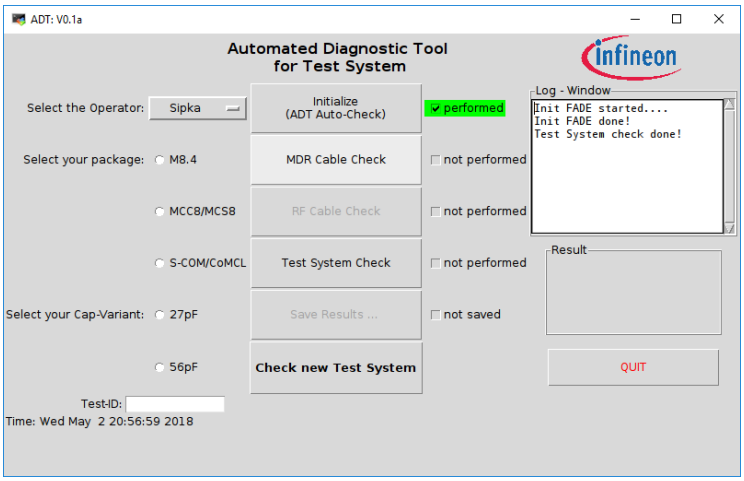

Figure 3.45: ADT Graphical User Interfacel

Figure 3.46 shows the GUI when the system check was performed and the result is ”PASS”.

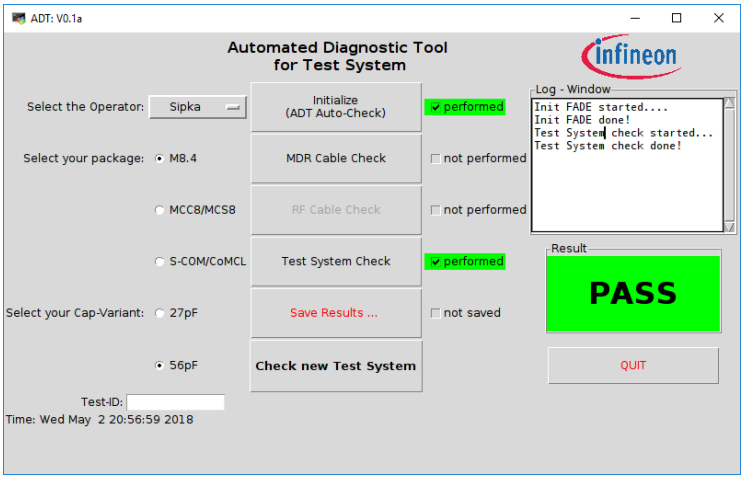

Figure 3.46: GUI on ADT test report is PASS

Unfortunately, during the writing of this thesis there was not enough time to implement the complete ADT software that is actually needed to successfully check the TS. Since the function such as miniVNA is only partially implemented, the verification and measuring of this part needs to be carried out manually.

4 Testing and Measurements

4.1 Current consumption and shunt resistor

This section describes the DC measurement and test results of the TS. In this testing and validation step, the TS device was tested under laboratory conditions. First, the current consumption (at +12 V supply for the relays) must be checked to find out which maximum current should be measured. The measured values will help to dimension appropriate shunt resistor. The setup is shown in Figure 4.1 and current consumption is measured with the DMM (Keithley 2000).

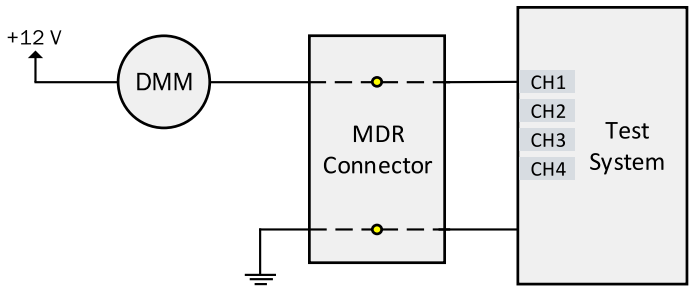

Figure 4.1: Overview of the test setup for current consumption by TS

In the first measurements method, single shot mode was performed. This means that only one measure value will be stored. However, this method is not sufficiently reliable for analysis purposes. For this measurement, the internal software tool from Infineon was used, in which the DMM is already implemented. To control the Keithley 2000 and evaluate the results for the current consumption measurements, the JavaScript was used. It was also expected that current consumption over a longer measurement period stays constant. These oscillations were needed to be checked by a more accurate analysis with a sweep method of 30 seconds, which later showed that the current is not constant.

More details of the current consumption are shown in Figure 4.2.

This figure obviously shows that the current consumption is not constant, contrary to the expectation. As the measurement was carried out over the sweep of 30 seconds, it was noticed that the current consumption is decreasing. This effect can be compared to a typical property of a positive temperature coefficient (PTC) resistor. PTC refers to materials that experience an increase in electrical resistance when their temperature is raised. This characteristic of the relay explains the unexpected decreasing current consumption with increasing temperature over the time.

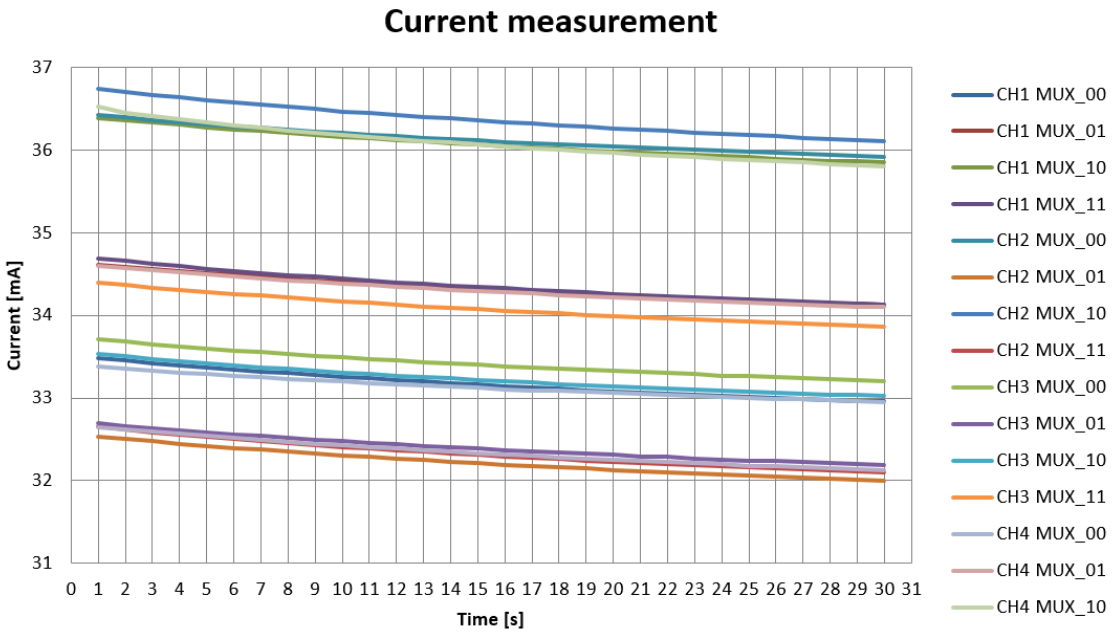

Figure 4.2: Overview of the current consumption by TS

After the multiple current consumption measurements, the next step is mean value calculation to find out the minimum as well as the maximum current consumption per channel of the TS. More details of the current consumption are shown in table 4.1.

Table 4.1: TS current consumption as mean value

TS	MUX_00 [mA]	MUX_01 [mA]	MUX_10 [mA]	MUX_11 [mA]
CH_1	33.17	34.33	36.07	34.36
CH_2	36.13	32.22	36.37	32.32
CH_3	33.41	32.40	33.23	34.08
CH_4	33.13	34.30	36.08	32.34

From Table 4.1 it can be concluded that through the active channel flows around 40 mA current. Bearing in mind the worst-case scenario that a TS demodulator could break down, a single channel can run a maximum of 160 mA. By knowing the value of current consumption, it was possible to calculate the Rshunt.

$$R_{shunt} = \frac{U_{shunt}}{I_{shunt}} = \frac{82\,mV}{160\,mA} = 0.512\,\Omega \tag{4.1}$$

4.2 Verification and Evaluation of ADT

In this section the simulation and laboratory measurement results will be presented and evaluated.

4.2.1 Testing of Communication Bus

Communication with the Raspberry Pi, the port expander and the current and voltage sensor has been verified. This section is devoted to a failure analysis and performance analysis of the ADT's I^2C bus. Special attention was devoted to the bus, so the whole system with its hardware and software could be stable and robust.

The communication bus is implemented using the PCA9306DC I^2C level shifter. This level shifter solves the problem with diferent IO levels on the ADT system. The communication bus has been tested between all modules and no problems were found. The following figure shows the scan results from the I^2C communication bus.

```
pi@raspberrypi:~ $ sudo i2cdetect -y 1
     0  1  2  3  4  5  6  7  8  9  a  
00: -- -- -- -- -- -- -- -- -- -- -- -
10: -- -- -- -- -- -- -- -- 18 -- 1a -
20: 20 21 22 23 24 25 26 27 -- -- -- -
30: -- -- -- -- -- -- -- -- -- -- -- -
40: 40 41 -- -- 44 45 -- -- 48 -- -- -
50: -- -- -- -- -- -- -- -- -- -- -- -
60: -- -- -- -- -- -- -- -- -- -- -- -
70: -- -- -- -- -- -- -- -- -- -- -- -
```

Figure 4.3: Overview of the I^2C scan all ICs available

The GUI application has been tested by connecting the system together. After the complete initialization procedure is done, the ADT system is ready for Test Procedure of the TS. The following figure shows the measurement results from the I^2C bus section. By using an oscilloscope to debug the bus communication an I^2C bus performance analysis has been made. During the performance analysis, the stability and reliability of the I^2C bus was extensively tested.

Communication with the Red Pitaya and the miniVNA was also tested. The communication on the ADT prototype proved to be successful as well.

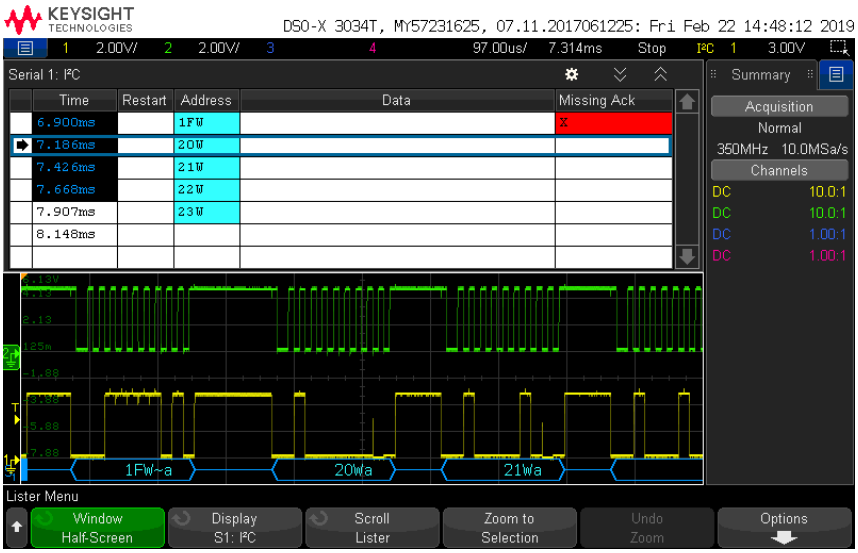

Figure 4.4: Example of a data transfer over the I^2C bus

The conclusion is that during the whole testing phase the communication bus provided very stable measurment results. The communication is functional and deprived of failures. Thus, the potential risk of an error during the communication between Raspberry Pi as a master and the module on slave devices is reduced to minimum.

4.2.2 Testing of Current and Voltage monitor

For the measurement accuracy of the sensors it is important to check the uncertainty of the sensor data. The INA226 measures the bus voltage and the differential voltage through the shunt resistor. The measurement results for the bus voltage with a resolution of 1.25 mV/bit are automatically stored. As well as the measurement result for the differential voltage of 2.5 μV/bit through the shunt resistor. However, the current and power measurement must be calibrated by the user as they are dependent on the value of the shunt resistor and the expected current. The calibration values can be calculated with the following equation:

$$CAL = \frac{0.00512}{C_{current_LSB} * R_{shunt}} \tag{4.2}$$

Where

$$C_{current_LSB} = \frac{MaximumExpectedCurrent}{2^{15}} \tag{4.3}$$

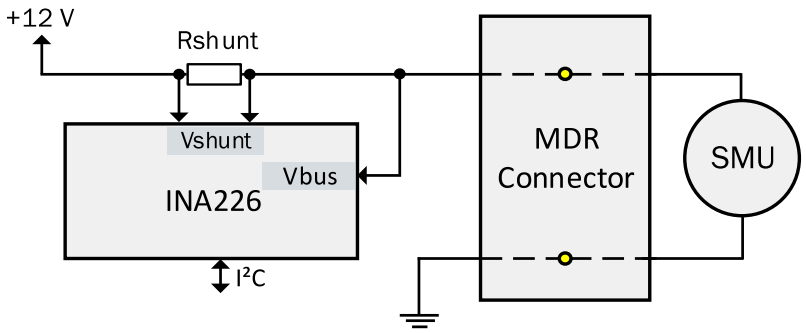

Figure 4.5: Test setup for current and voltage monitoring

To measure how accurate INA226 is, a test setup shown in Figure 4.5 was created. For the results to be as accurate as possible, the devices SMU and DMM were calibrated. In this case, the SMU is a load, connected to the ADT by the MDR cable. The measuring range was from 1 mA to 130 mA. To determine the exact drop voltage on the shunt resistor, the DMM Keithley 2000 was used. For the analysis, two different types of resistors were used. R= 0.5 Ω was chosen because the maximal consumption current is 160 mA, whereas Rshunt=0.39 Ω was chosen to see how much degree of accuracy the INA226 has.

In the table below, the measured values are presented. *Iset* is the given current, *Vmeas* is the bus supply voltage. DMM is Keithley 2000 multimeter that measures the (*Vdifm*) differential voltage across the shunt resistor, providing a value that can be compared with INA226. The last three columns represent the measured values for INA226 for the first value Rshunt= 0.5 Ω.

Table 4.2: INA226 (Rshunt= 0.5 Ω) current and bus voltage compared with reference measurement

SMU		DMM	INA226			
Iset	Vmeas	Vdifm	Vbus	Isense	Vdif	Rshunt
mA	V	mV	V	mA	mV	mΩ
1	12.06	0.51	12.07	1.02	0.51	500.00
5	12.04	2.52	12.06	5.04	2.52	499.55
10	12.02	5.03	12.05	10.05	5.03	499.93
15	12.00	7.54	12.04	15.08	7.54	499.95
20	11.97	10.05	12.03	20.10	10.05	499.96
25	11.95	12.56	12.02	25.12	12.56	499.91
30	11.93	15.07	12.01	30.14	15.07	499.94
35	11.90	17.57	12.00	35.16	17.58	499.95
40	11.88	20.08	11.99	40.18	20.09	499.94
45	11.86	22.60	11.98	45.20	22.60	499.97
50	11.83	25.10	11.97	50.22	25.11	499.95
100	11.60	50.19	11.86	100.43	50.21	499.98
130	11.46	65.36	11.79	130.76	65.39	500.05

The second table is filled with the measured values for the second chosen value of Rshunt= 0.39 Ω.

Table 4.3: INA226 (Rshunt= 0.39 Ω) current and bus voltage compared with reference measurement

SMU		DMM	INA226			
Iset	Vmeas	Vdifm	Vbus	Isense	Vdif	Rshunt
mA	V	mV	V	mA	mV	mΩ
1	12.06	0.40	12.07	1.01	0.40	390.95
5	12.05	1.96	12.06	5.02	1.96	390.13
10	12.02	3.91	12.05	10.02	3.91	389.73
15	12.00	5.86	12.04	15.02	5.86	390.01
20	11.99	7.81	12.03	20.03	7.81	389.92
25	11.96	9.76	12.02	25.03	9.76	389.96
30	11.94	11.71	12.01	30.04	11.71	389.87
35	11.92	13.66	12.00	35.04	13.66	389.93
40	11.90	15.61	11.99	40.04	15.61	389.91
45	11.87	17.56	11.98	45.04	17.56	389.95
50	11.85	19.51	11.97	50.05	19.52	389.95
100	11.64	39.01	11.87	100.07	39.02	389.97
130	11.50	50.79	11.81	130.29	50.81	389.94

DMM has a typical voltage measurement error of 0.025 % and the INA226 voltage measurement was computed to be 0.044 %. DMM has a typical current error of 0.15 % and the typical error of the INA226 current measurement is 1.0 % or ±1 mA.

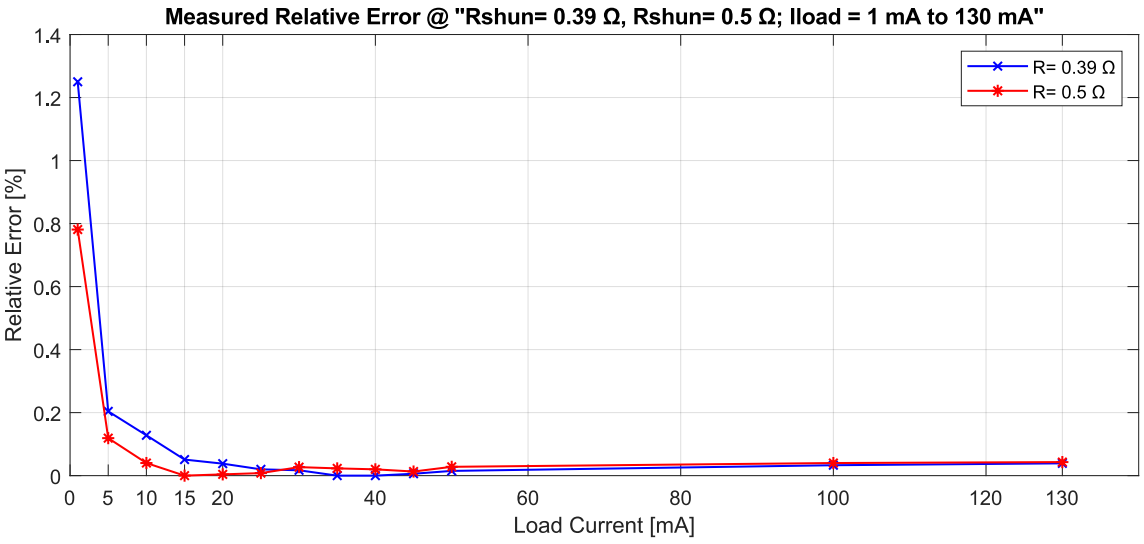

Figure 4.6: Measured Relative Error @ "Rshun= 0.39 Ω, Rshun= 0.5 Ω; Iload = 1 mA to 130 mA"

Figure 4.6 shows that INA226 fulfills the requirements from the section 3.1. It also can be seen that in the range up to 20 mA, Rshunt= 0.5 Ω, measures more accurately. As the Load Current is increasing in the range above 40 mA, the relative error is almost the same for both different values of Rshunt (0.39 Ω and 0.5 Ω).

4.2.3 Testing of RF selector

To ensure that the miniVNA together with the RF selector meets our ADT requirements, the results measured from the miniVNA were compared with Bode 100. A vector network analyzer Bode 100 from Omicron Electronics (frequency range 1 Hz – 40 MHz) was used as a reference device for the impedance measurements. [5] The miniVNA is firstly calibrated using the (OPEN-SHORT-LOAD) calibration routine and calibration files are created using the miniVNA software. The S11 measurement of the miniVNA PRO was then compared to the S11 measurement of the Bode 100 in order to verify the calibration that was performed correctly on the miniVNA PRO. Both, the real and imaginary part of the S11 measurement have a fairly similar measurement. This means that the PCB routing is not a limiting factor for the measurement.

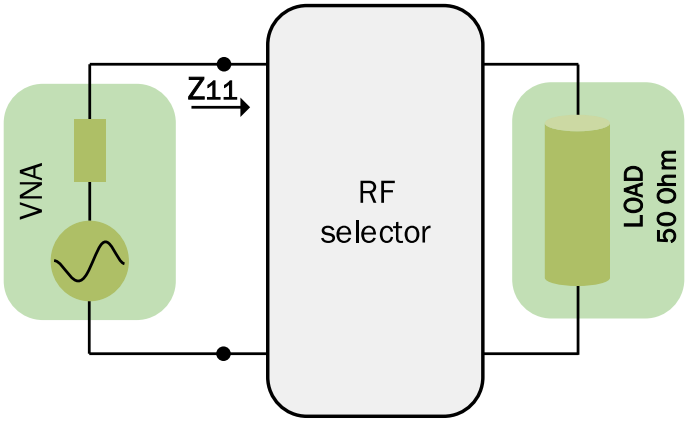

Figure 4.7: Overview of the test setup for RF selector

As next step, the PCD reader antenna provided by Infienon was used as a load. The antenna is connected to the output of the RF selector, and the test setup is shown in Figure 4.7.

To determine the effect of the PCB on the whole system, two variations were compared during this measurement. The first measurement is to calibrate the VNA (connected to Port 1) before the RF selector, to carry out the measurement for each port from P4 to P8. Other variant is to calibrate the VNA on RF selector output ports. The measured values of PCD reader antenna with BODE 100 are compared with these two above mentioned methods which are shown in the Figure 4.8 presented in a Smith chart plot. The diagram clearly states the influence of the RF selector on the whole system. Since PCB is designed with controlled impedance, this parameter clearly shows how much deviation from the target value of 50 Ω exists.

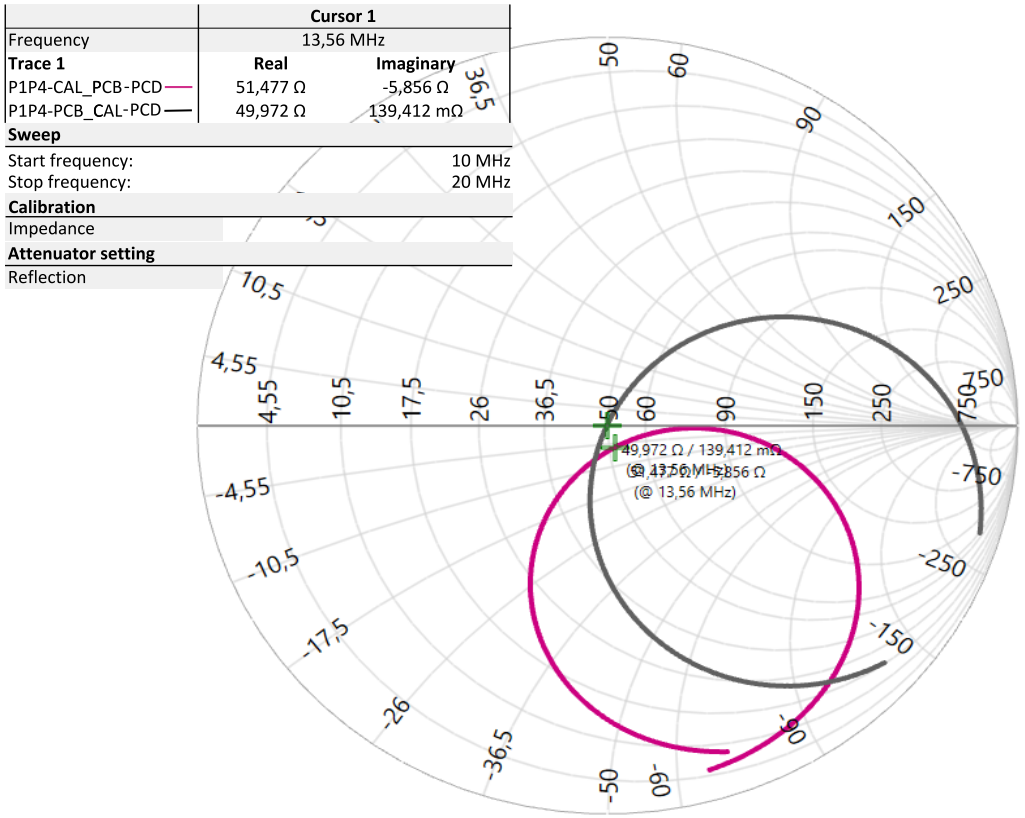

Figure 4.8: Smith Chart showing PCD antenna impedance at 13.56 MHz, VNA is calibrated before the RF selector (black) and VNA is calibrated on RF selector output ports (red)

Next measurement is performed to compare the measured values of the PCD reader antenna with the BODE 100 to the miniVNA. The calibration was performed before the measurement, so this time the RF selector is compensated with (OPEN-SHORT-LOAD) calibration. That means that focal point of the measurement is placed on the output ports P4 to P8. The S11 output of the RF selector impedance measurement is shown in table 4.4 for both the BODE 100 and the miniVNA PRO.

Table 4.4: Comparison of BODE 100 and miniVNA PRO impedance measurement

	BODE 100		miniVNA	
Port	Re [Ω]	Im [mΩ]	Re [Ω]	Im [mΩ]
P1P4	50.014	189.647	50.20	421.00
P1P5	49.972	139.412	49.90	100.0
P1P6	50.113	338.76 m	50.10	306.0
P1P7	50.216	663.168	49.90	711.0

4.2.4 Simulation of RF selector

Figure 4.9 shows the PCB of the RF selector and Port labels from subsection 3.2.1.4. Port 1 is an input for VNA, whereas the ports from P4 to P7, and from P8 to P11 are outputs. As stated in the subsection 3.2.1.4, there are two types of design topologies. First variant is that impedance is controlled and trace lengths are matched. Second variant is that impedance is controlled and the length of the traces is without exact matching. To determine which of these topologies has a better performance, the simulation was carried out in HFSS tool.

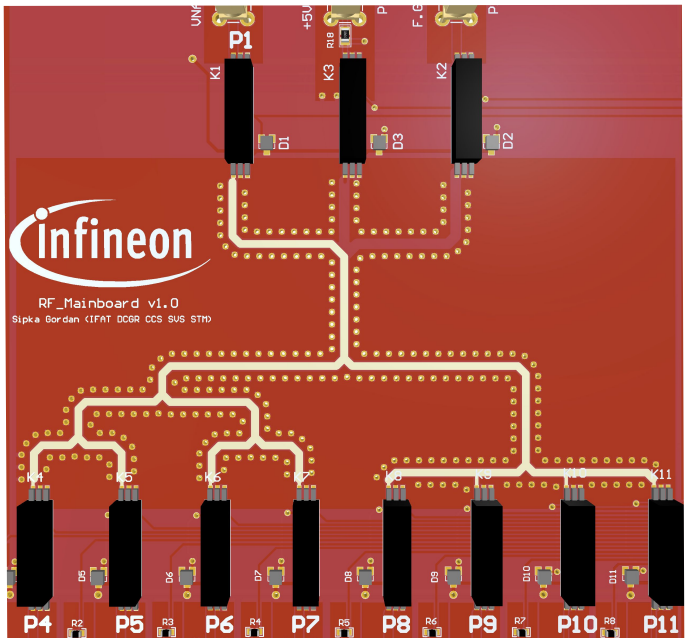

Figure 4.9: Overview of the PCB port labeling

The results of the impedance measurement for the port P1 as an input and P4 to P7 as well as P8 to P11 as output ports are illustrated in the Figure 4.10 This Figure illustrates different curves of the impedance Z. As the frequency increases, the size of the impedance decreases. This behavior was predictable due to the physical properties of a PCB. The point at 13.56 MHz is interesting since the difference between the tested outputs is about $\pm 1\ \Omega$.

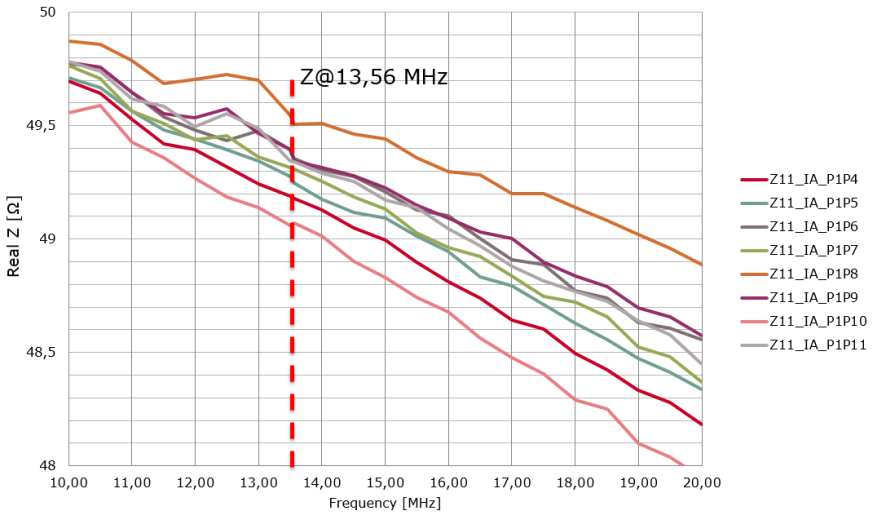

Figure 4.10: Results showing PCB impedance for each Port (port 4 up to port 11) for frequency sweep from 10 MHz to 20 MHz

In the following Figure, a more detailed presentation of this simulation at 13.56 MHz is presented. Both, real and imaginary values are also presented. The real overview clearly shows that there is no big difference between the two tested topologies and that both groups have close target values of 50 Ω. Concerning the imaginary part, it is evident that all ports have negative value in the range of -3.5 Ω.

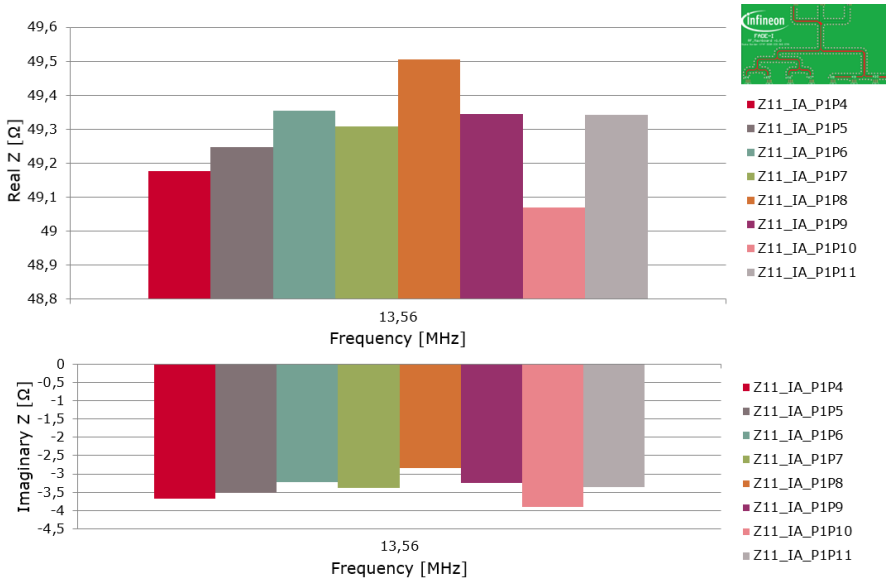

Figure 4.11: Results showing PCB impedance for each Port (port 4 up to port 11) at 13.56 MHz

By comparing the values of the measurement and the simulation, it is shown that the deviation is not bigger than 2 % at 13.56 Hz.

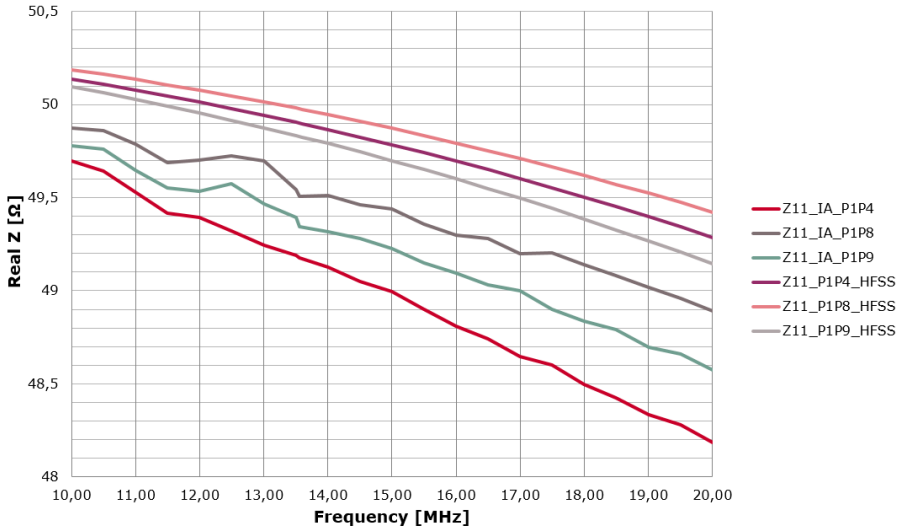

Figure 4.12: Comparison between simulation and measurement results for impedance measurement

The measurement and simulation have showed that there is no big difference between prototype board and the stimulation. Ragarding the topology, the topology where impedance is controlled, and trace lengths is matched will be used furtherly.

It can be concluded that during the whole testing phase the PCB did not show any weakneesses regrading the measurement results. Digital logic together with the relays operated without any problems. The miniVNA demonstrated stability and preciseness during the measurements. Since miniVNA is not an open source, it is not easy to integrate it into a software. However, this product offers a software with headless application (no graphical user interface). The application itself was functional, but the data transfer was very slow. With future redesigning, a special attention needs to be given in choosing the VNA. This section tested the Red Pitaya, i.e. its utility as a functional generator. With the use of Python script, there were no problems with its running.

4.2.5 IV Mainboard

Unfortunately, during this thesis, there was not enough time to validate a complete set of ADT hardware and software that is actually needed to successfully finalize ADT. However, some improvements can be made for future tasks. These future work packages are presented and described in next section.

5 Conclusion and Outlook

5.1 Conclusion

Nowadays, the companies from the semiconductor industries must provide themselves a quality assurance for their products. In order to cut manufacturing time and expenses in the final testing of the product, RFID technologies proved to be remarkably vital. In this regard, this master thesis offers a unique design and implementation of the Automated Diagnostic Tool, whose general purpose is to check verification and calibration of the Test System, which consists of important hardware parameters. Together with the software requirements and measuring instruments necessary for the setup test, this thesis also provides a full design of the ADT's enclosure. The applicability of the Automated Diagnostic Tool is subsequently confirmed through practical application and meticulous analysis. Its general purpose, alongside verification and calibration is additionally focused on root cause failure analysis and what is more important – a solution provider for the identified errors. The developed ADT system is separated into three significant design segments: hardware, enclosure and software. Raspberry Pi as a board computer was a necessary device for ADT stand-alone configuration. Red Pitaya was used as a measuring device which provided the oscilloscope and signal generator. To ensure a high level of flexibility in advance, the ADT system was developed as modular as possible with common standards. These are separated into five modules: MDR Mainboard, MDR Cable-check, RF selector, IV Mainboard and RP Adapter. To design a fully functional prototype as industrial equipment, it was necessary to develop ADT enclosure system. Third crucial segment of the ADT design was its software configuration. To allow Red Pitaya connection and to enable the control of the oscilloscope and the function generator, as well as to allow miniVNA connection with a basic function, Python as a programming language was used for Raspberry Pi and GUI was implemented with TKinter. To be operational, the ADT system software required three main processes - initialization, data acquisition and data reporting. The testing of the ADT was carried out in laboratory conditions where GUI application has been tested by connecting the whole system together. In that way, the ADT system was ready for Test Procedure of the Test System.

5.2 Outlook

The research presented in this thesis has opened a number of research lines that should be explored in the future. Any future improvement on the ADT and test system can certainly reduce failure searching times. Failures can be found and diagnosed very easily,

because repair instructions are being shown on the display, as well as on a remote dashboard available to the expert support. Additionally, also reduced will be the time for supplementary measurement cycles and high maintenance costs. Due to such improved maintenance, the lowering of the shipping costs will also be directly affected.

The Automated Diagnostic Tool should support secure remote calibration of the test system, in addition to remote diagnosis of TS and contactless reader failures. To build a meaningful remote diagnosis and maintenance support, several innovative development works are necessary, which can be updated in the future work such as calibration features that needs to be extended to be able to display more detailed error reports as well as repair instructions for locally present users. Future research should examine strategically to secure the transferred data. Thus, the system needs to be equipped with trusted computing functionalities. Looking forward, further attempts could be proved quite beneficial to the whole area of ADT test system performance.

Appendix A

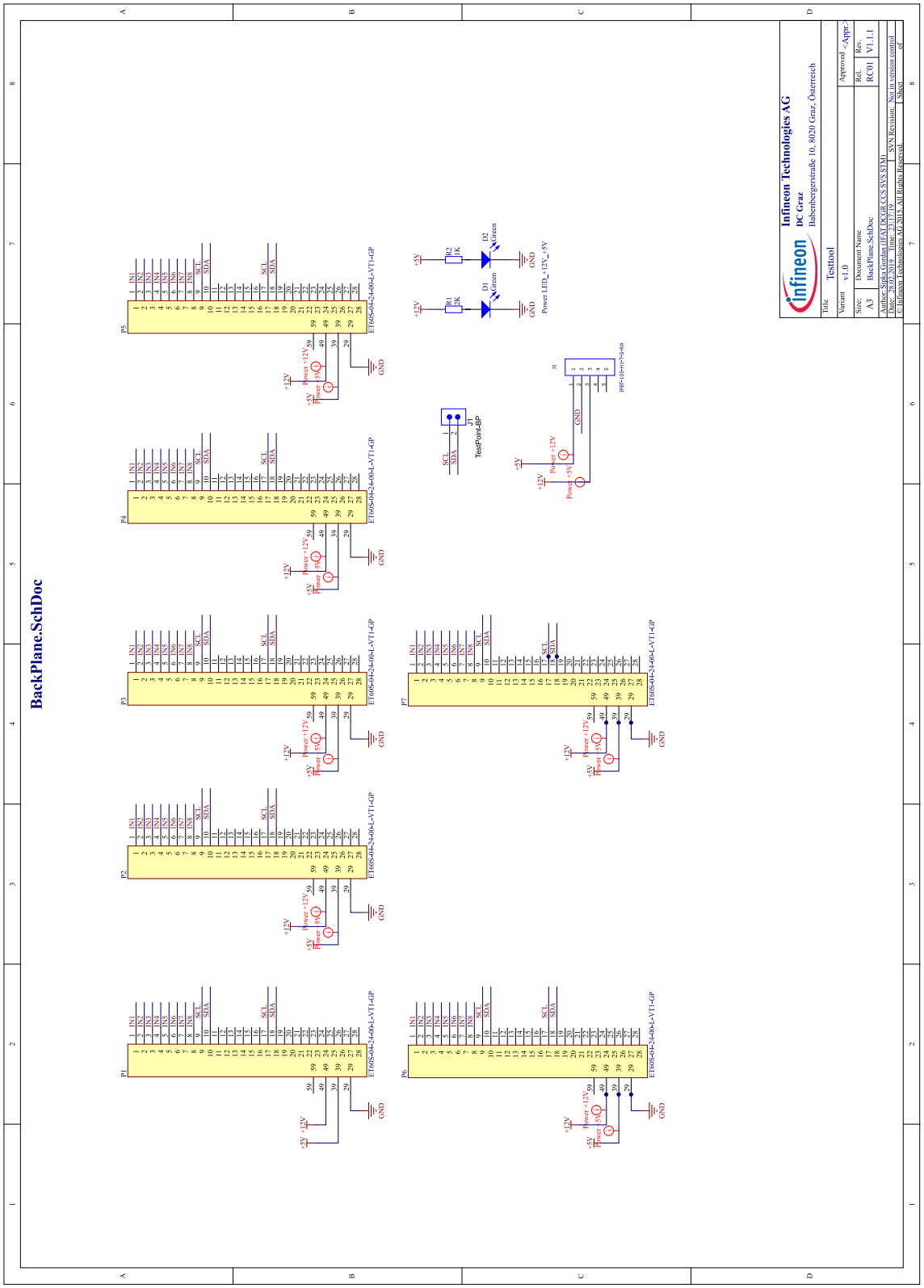

Figure .1: Backplane SCH

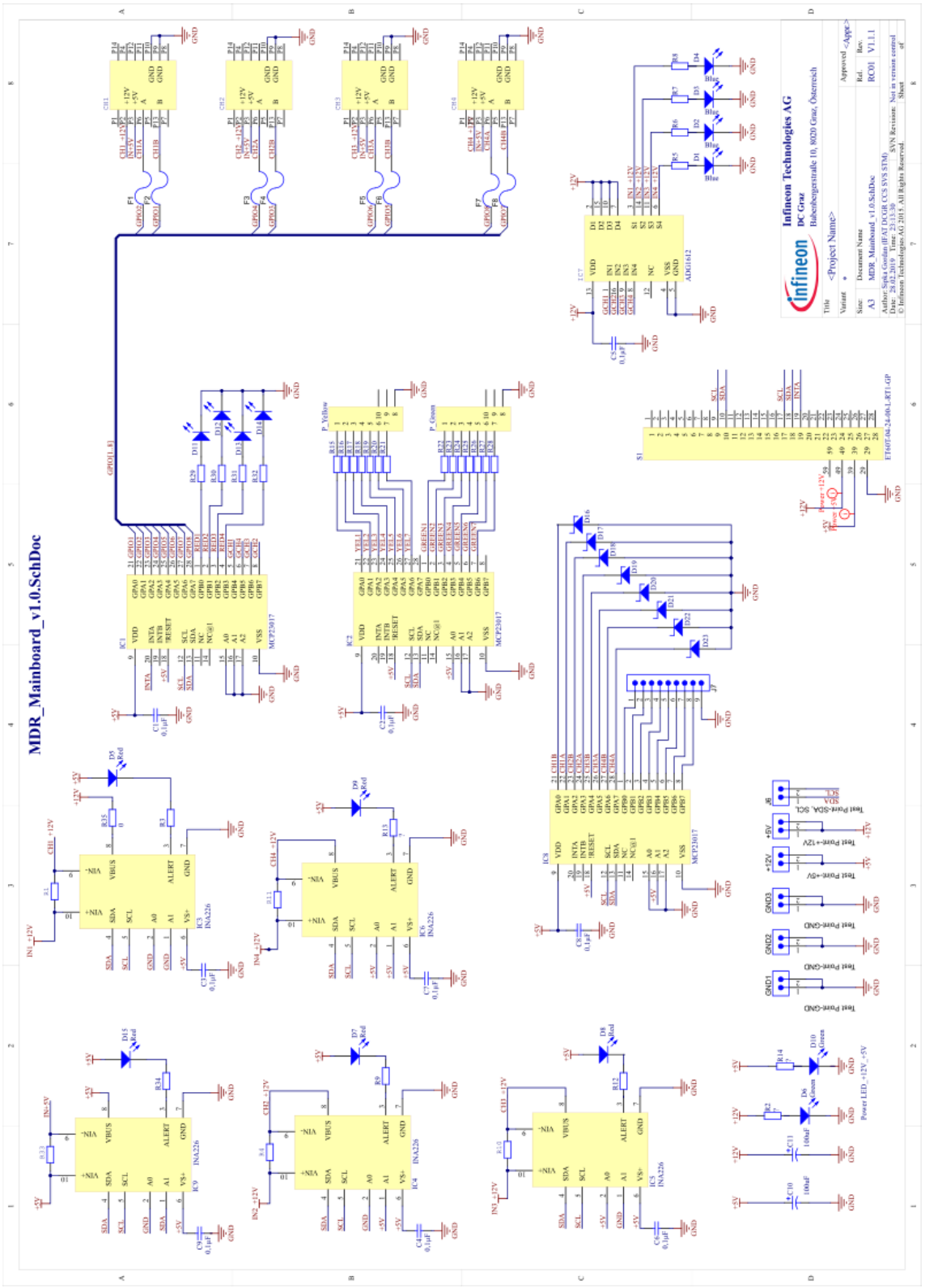

Figure .2: MDR Mainboard SCH

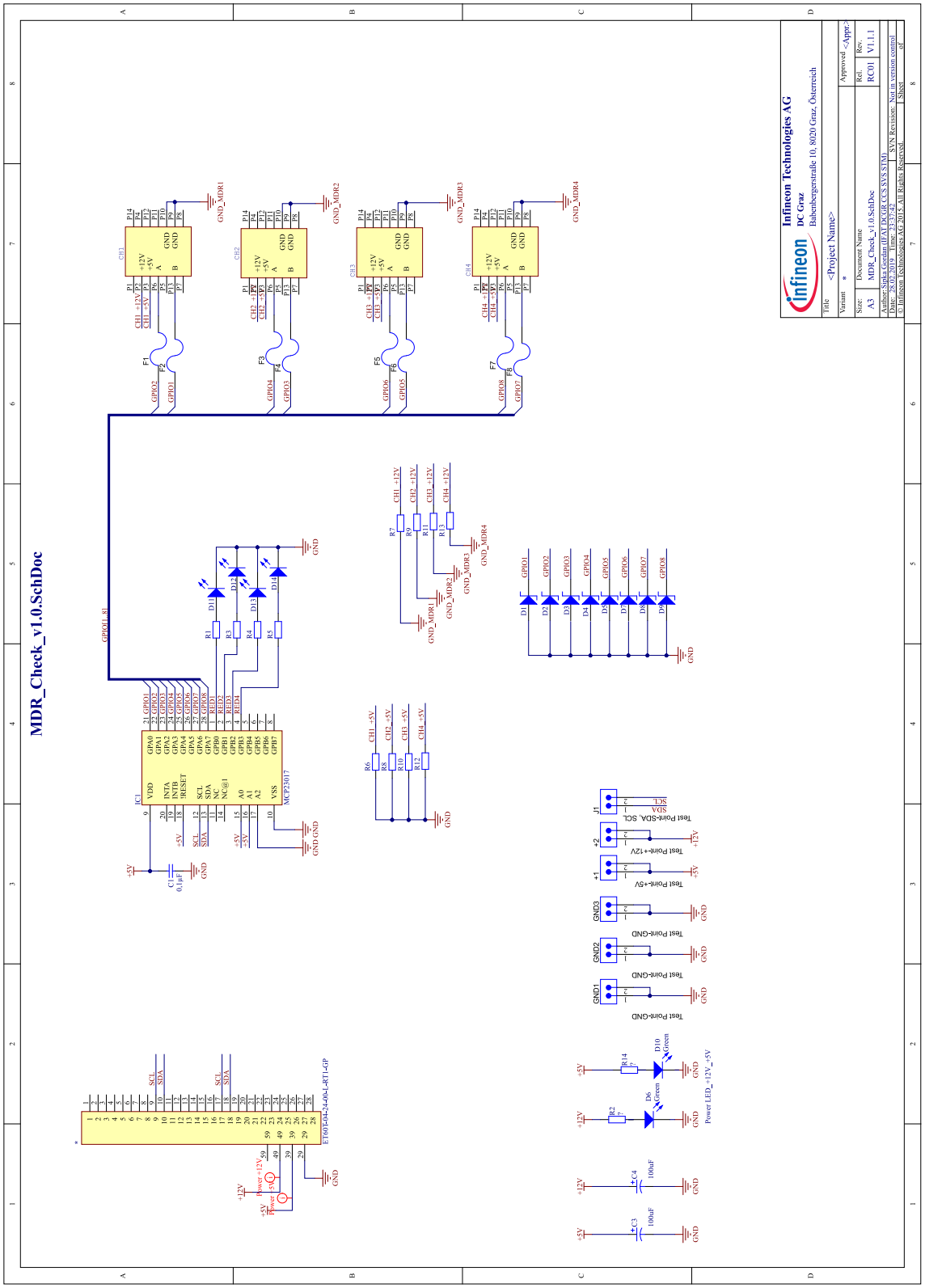

Figure .3: MDR cable SCH

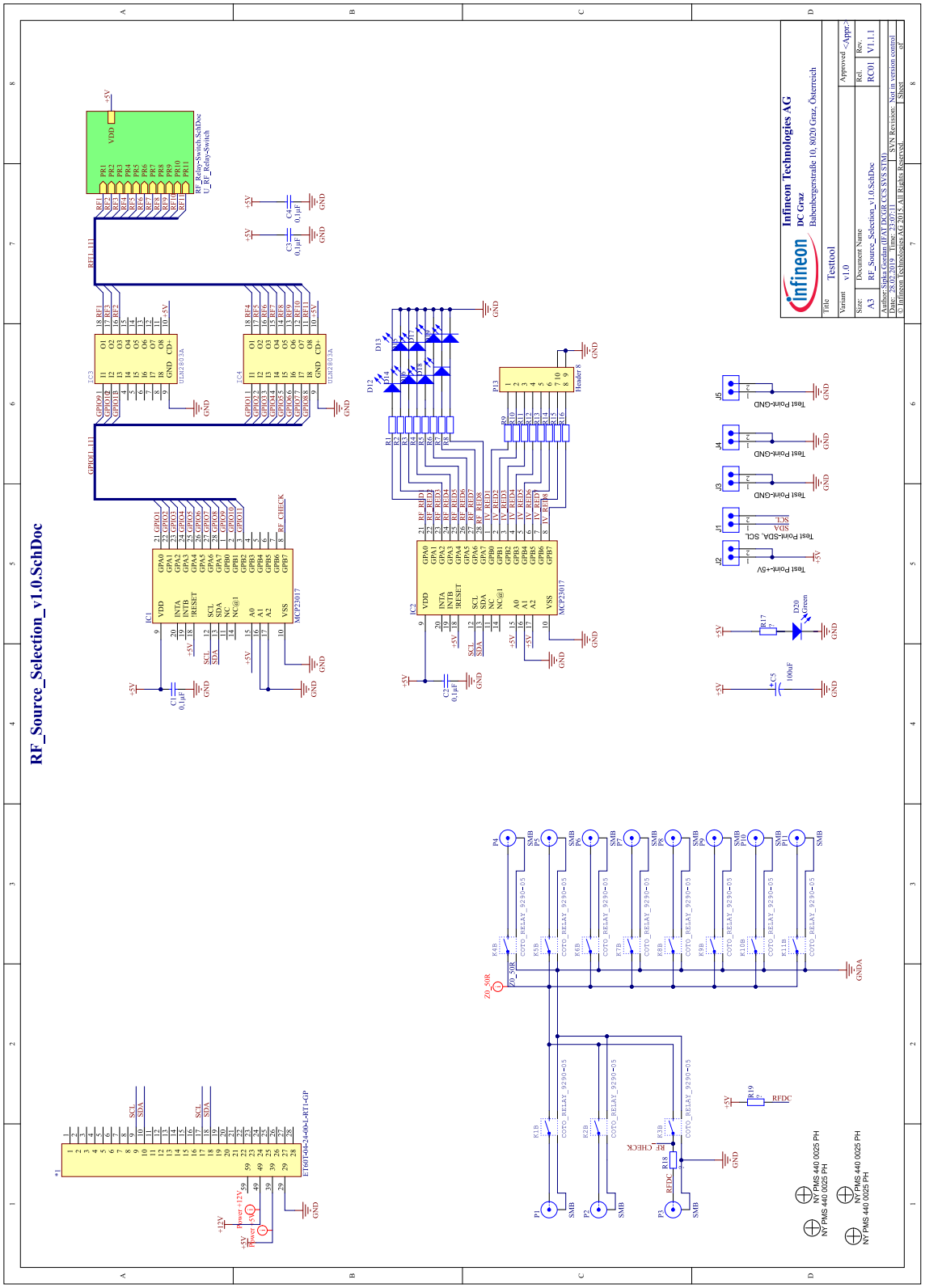

Figure .4: RF selector SCH

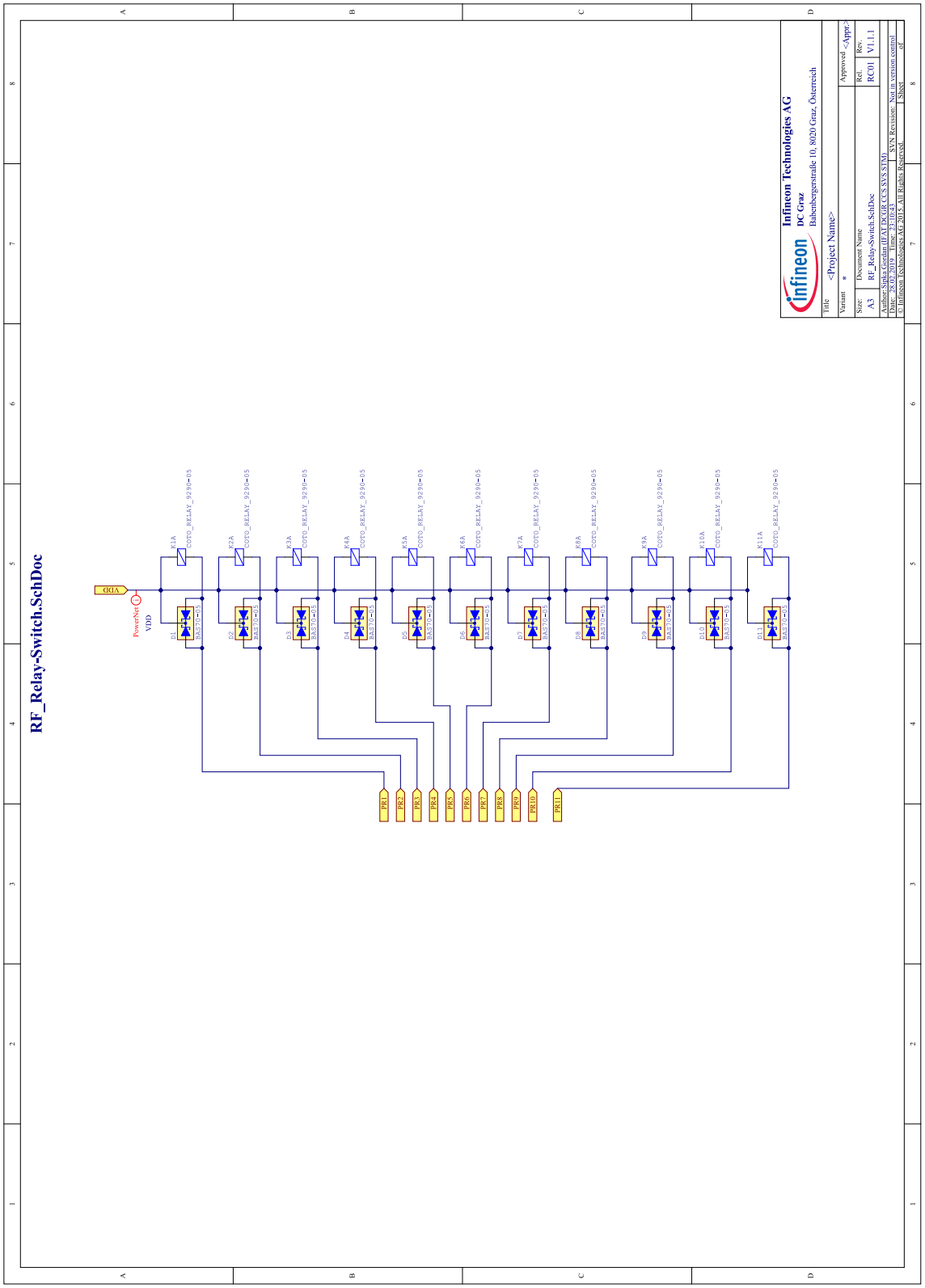

Figure .5: RF selector SCH

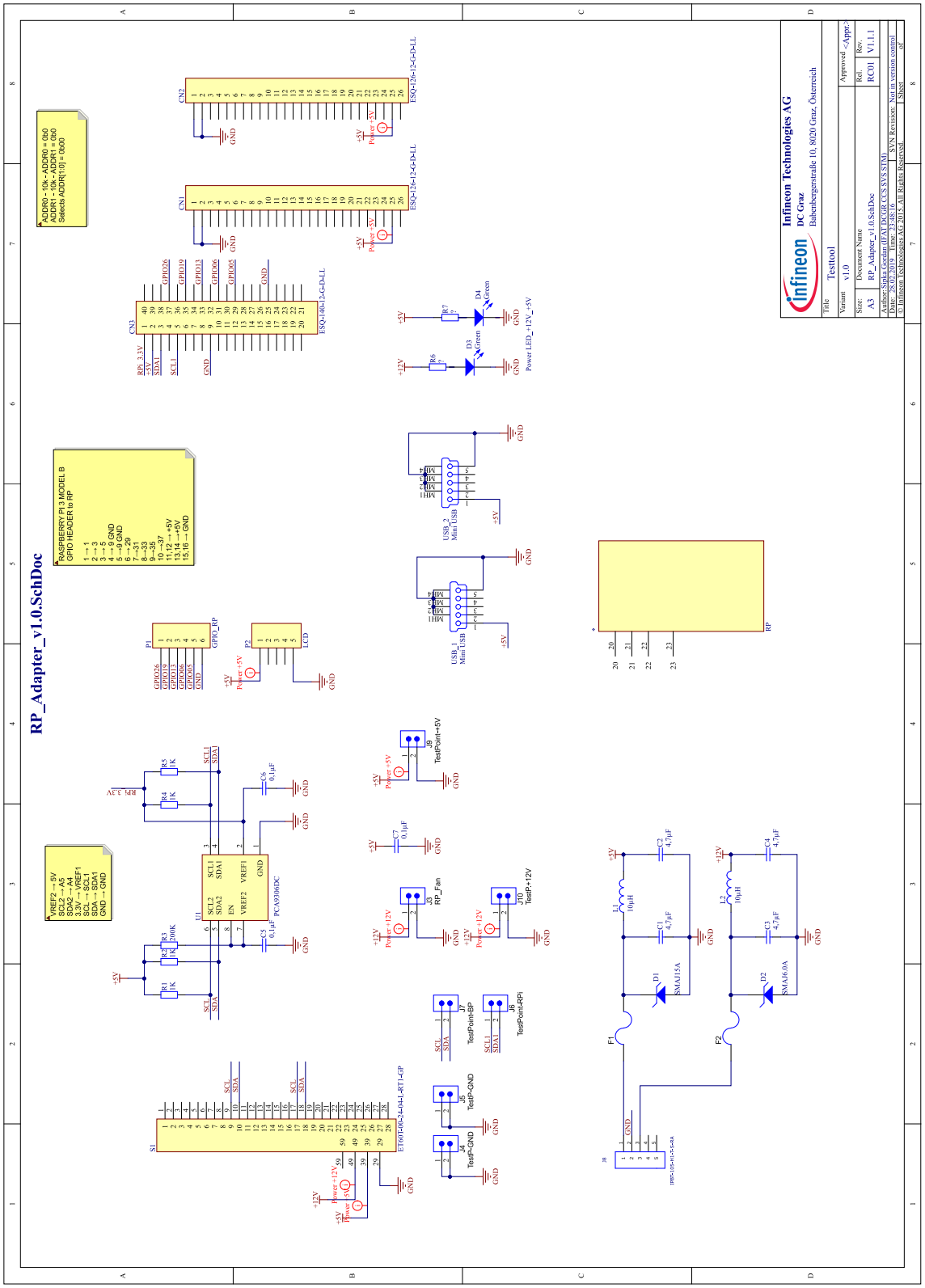

Figure .6: RP adapter SCH

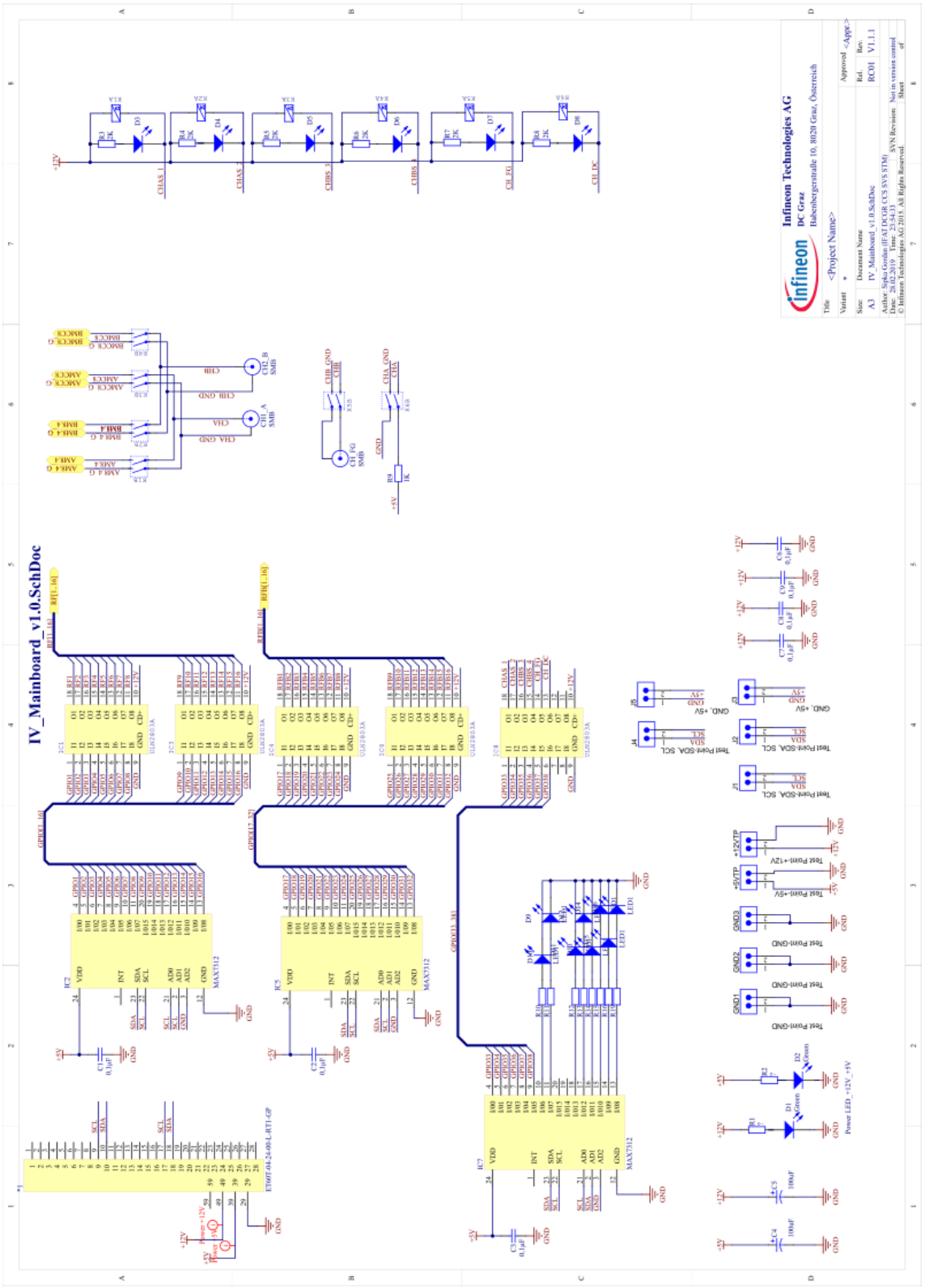

Figure .7: IV mainboard SCH

Bibliography

[1] *Adafruit's Raspberry Pi Lesson 4. GPIO Setup*. [Online; accessed 31. Jan. 2019]. Sept. 2018. URL: https://cdn-learn.adafruit.com/downloads/pdf/adafruits-raspberry-pi-lesson-4-gpio-setup.pdf?timestamp=1551010749 (cit. on p. 10).

[2] *Analog Devices ADG1612BRUZ*. [Online; accessed 31. Jan. 2019]. Jan. 2019. URL: https://www.analog.com/media/en/technical-documentation/data-sheets/adg1611_1612_1613.pdf (cit. on p. 24).

[3] *Antenna design guide*. [Online; accessed 24. Feb. 2019]. Feb. 2018. URL: https://www.nxp.com/docs/en/application-note/AN11706.pdf (cit. on p. 15).

[4] *BOARD-TO-BOARD CONNECTORS*. [Online; accessed 31. Jan. 2019]. Jan. 2019. URL: http://suddendocs.samtec.com/literature/samtec-micro-rugged-design-guide.pdf (cit. on p. 20).

[5] *Bode 100*. [Online; accessed 24. Feb. 2019]. Feb. 2017. URL: https://www.omicron-lab.com/fileadmin/assets/Bode_100/Manuals/Bode-100-User-Manual-ENU10060503.pdf (cit. on p. 57).

[6] SCPI Consortium. *Standard Commands for Programmable Instruments (SCPI), Mai 1999*. May 1999. URL: http://www.ivifoundation.org/docs/scpi-99.pdf (visited on 01/09/2019) (cit. on p. 12).

[7] I. Dogan. *Red Pitaya for Test and Measurement*. Elektor Publishing, 2016 (cit. on p. 11).

[8] *EXTreme Ten60Power RIGHT-ANGLE POWER/SIGNAL HEADER*. [Online; accessed 31. Jan. 2019]. Jan. 2019. URL: http://suddendocs.samtec.com/catalog_english/et60t.pdf (cit. on p. 22).

[9] *EXTreme Ten60Power SOCKET*. [Online; accessed 31. Jan. 2019]. Jan. 2019. URL: http://suddendocs.samtec.com/catalog_english/et60s.pdf (cit. on p. 20).

[10] K. Finkenzeller. *RFID Handbook: Fundamentals and Applications in Contactless Smart Cards, Radio Frequency Identification and Near-Field Communication*. third edition. John Wiley & Sons, 2010 (cit. on pp. 3, 4).

[11] Raspberry Pi Foundation. *Raspberry Pi — Teach, Learn, and Make with Raspberry Pi*. 2018. URL: https://www.raspberrypi.org (cit. on pp. 6, 7).

[12] J. Franz. *EMV Störungssicherer Aufbau elektronischer Schaltungen*. Springer-Verlag, 2013 (cit. on p. 38).

[13] *Hardware Guide for miniVNA PRO*. [Online; accessed 24. Feb. 2019]. July 2012. URL: http://www.wimo.de/download/minivnapro_Hardware%20guide_english.pdf (cit. on p. 14).

[14] *I2C-bus specification and user manuall*. [Online; accessed 31. Jan. 2019]. Apr. 2014. URL: https://www.nxp.com/docs/en/user-guide/UM10204.pdf (cit. on pp. 7–9).

[15] *INA226 High-Side or Low-Side Measurement,Bi-Directional Current and Power Monitor with I2C Compatible Interface*. [Online; accessed 31. Jan. 2019]. Jan. 2019. URL: http://www.ti.com/lit/ds/symlink/ina226.pdf (cit. on p. 25).

[16] H. Lehpamer. *RFID Design Principles*. second edition. Artech House, 2012 (cit. on p. 4).

[17] H. Lienig. *Elektronische Geraetetechnik*. Springer-Verlag, 2014 (cit. on p. 38).

[18] *MCP23017 16-Bit I2C I/O Expander with Serial Interface*. [Online; accessed 31. Jan. 2019]. Jan. 2019. URL: http://ww1.microchip.com/downloads/en/DeviceDoc/20001952C.pdf (cit. on pp. 23, 25).

[19] *MP300 CL3*. [Online; accessed 24. Feb. 2019]. Sept. 2018. URL: https://www.microprossa.com/Manufacturing-testers-WPC-Qi-production-tool-mp300-cl3-64-p (cit. on p. 4).

[20] *Network Analyzer Basics*. [Online; accessed 24. Feb. 2019]. July 2014. URL: http://literature.cdn.keysight.com/litweb/pdf/5965-7917E.pdf (cit. on p. 13).

[21] *Red Pitaya STEMlab Documentation*. [Online; accessed 24. Feb. 2019]. Feb. 2019. URL: https://media.readthedocs.org/pdf/redpitaya/latest/redpitaya.pdf (cit. on p. 12).

[22] *vna/J 2.6.7 Users guide*. [Online; accessed 24. Feb. 2019]. Sept. 2010. URL: http://www.sp2swj.sp-qrp.pl/SP3SWJ/MAX6/PROGRAM/VNA-J/vnaJ_UserGuide_2_6_7.pdf (cit. on pp. 14, 15).